

Fingerprinting Generative Adversarial Networks

Guanlin Li, Guowen Xu, Han Qiu, Shangwei Guo, Run Wang, Jiwei Li, Tianwei Zhang,
Rongxing Lu, *Fellow, IEEE*

Abstract—Generative Adversarial Networks (GANs) have been widely used in various application scenarios. Since the production of a commercial GAN requires substantial computational and human resources, the copyright protection of GANs is urgently needed. In this paper, we present the *first* fingerprinting scheme for the Intellectual Property (IP) protection of GANs. We break through the stealthiness and robustness bottlenecks suffered by previous fingerprinting methods for classification models being naively transferred to GANs. Specifically, we innovatively construct a *composite deep learning model* from the target GAN and a classifier. Then we generate fingerprint samples from this composite model, and embed them in the classifier for effective ownership verification. This scheme inspires some concrete methodologies to practically protect the modern GAN models. Theoretical analysis proves that these methods can satisfy different security requirements necessary for IP protection. We also conduct extensive experiments to show that our solutions outperform existing strategies.

Index Terms—Fingerprint, generative adversarial network, adversarial example

I. INTRODUCTION

GENERATIVE Adversarial Networks (GANs) [1] are used in various applications, e.g., image and audio synthesis [2], [3], attribute editing [4], text-to-image translation [5]. A well-trained GAN model (especially the generator) is regarded as the core Intellectual Property (IP) due to two reasons [6]. First, to cope with complicated tasks and datasets, modern GAN models are designed to be more sophisticated. For instance, BigGAN [7] has 8.32 billion floating-point operations (BFLOPs) while SAGAN [8] has 9.18 BFLOPs. Training such a production-level GAN model usually requires a large amount of computing resources, valuable data, and human expertise. Second, GAN models are adopted in many applications with huge commercial values, such as image/video filters in TikTok [9], anime character maker MakeGirlsMoe [10], and Beauty Cam [11]. Therefore, the model vendors have strong motivations to protect such assets, and prevent the malicious model buyers or customers from abusing, copying or redistributing the models without authorization.

Guanlin Li, Guowen Xu, and Tianwei Zhang are with the School of Computer Science and Engineering, Nanyang Technological University, Singapore. (E-mail: guanlin001@e.ntu.edu.sg; guowen.xu@ntu.edu.sg; tianwei.zhang@ntu.edu.sg)

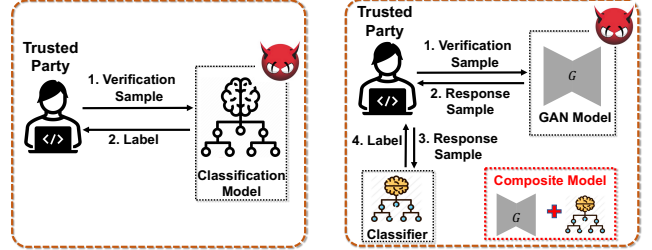
Han Qiu is with the Institute for Network Sciences and Cyberspace, Beijing National Research Center for Information Science and Technology, Tsinghua University, China. (E-mail: qiuhuan@tsinghua.edu.cn)

Shangwei Guo is with the School of Computer Science and Engineering, Chongqing University, China. (E-mail: gswei5555@gmail.com)

Run Wang is with the School of Computer Science and Engineering, Wuhan University, China. (E-mail: wangrun@whu.edu.cn)

Jiwei Li is with the School of Computer Science and Engineering, Zhejiang University, China and Shannon.AI. (E-mail: jiwei_li@shannonai.com)

Rongxing Lu is with the Faculty of Computer Science, University of New Brunswick, Canada. (E-mail: rlul@unb.ca)



(a) Classification Model

(b) GAN Model (ours)

Fig. 1: Fingerprinting different kinds of models.

Existing IP protection methods for deep learning models can be roughly divided into two categories. (1) *Watermarking*: the model owner embeds carefully-crafted watermarks into the target model by a parameter regularizer [12] or backdoor data poisoning [13]–[16]. Later, the watermarks can be extracted from the model parameters or output as the ownership evidence. (2) *Fingerprinting*: the model owner generates unique sample-label pairs that can exclusively and exactly characterize the target model (Fig. 1a). Common approaches [17]–[21] adopt **adversarial examples** to identify such fingerprint examples. Compared to watermarking, fingerprinting does not need to make modifications on the target model. Hence, it can better preserve the performance of the target model [17], [21]. It also shows more applicability and convenience, especially for some scenarios where the model owner does not have the right or capability to modify the models. Due to these advantages, fingerprinting is a more promising method for IP protection of deep learning models, and we focus on this strategy in this paper.

However, simply extending prior fingerprinting solutions from classification models to GAN models can cause some issues. (1) *Persistency*: adversarial examples against GANs are more sensitive to the changes in the model or input-output. So it is easier for an adversary to invalidate such fingerprints by slightly transforming the models or data samples. (2) *Stealthiness*: the adversarial output from a GAN model can be more anomalous than the adversarial label from a classification model, giving the model thief opportunities to detect the fingerprint and then manipulate the verification results. Experiments in Section VI quantitatively demonstrate these limitations. It is necessary to design a fingerprinting scheme dedicated to GAN models.

We propose the *first* fingerprinting scheme to protect the IP of image-to-image translation GAN models. The key innovation of our scheme is a *composite deep learning model* constructed from the target GAN model and a classifier (shown in Fig. 1b). Specifically, to make the ownership verification *stealthier*, we aim to design a set of fingerprints, whose input samples and output samples from the target model are visually indistinguishable from normal ones. With this requirement, it

seems impossible for the model owner to detect the plagiarism, as prior solutions require the output of the plagiarized model has large divergence from the ground truth. To address this issue, we propose to employ a classifier that can accurately identify the output from the plagiarized model, and assign a unique label to it. The introduction of the classifier can also enhance the *persistence* of the fingerprints: although the model owner is not permitted to change the target GAN model, he can freely modify the classifier to better recognize the fingerprint output. This benefit cannot be achieved in prior solutions [17]–[20].

Based on this scheme, we provide three concrete designs that can practically protect the IP of GAN models. In the first method (CFP-AE), the model owner can produce a set of fingerprint samples (i.e., verification samples), whose outputs from the target model are adversarial examples exclusively for the owner’s classifier. In the second and third methods (CFP-iBDv1, CFP-iBDv2), the target model’s responses to the fingerprint samples are designed to be invisible backdoor samples [22], which can activate the backdoor embedded in the classifier to produce unique labels. We leverage the Triplet Loss [23] and fine-grained categorization [24], [25] techniques to design novel loss functions, which can implant the backdoor into the classifier for better security and efficiency.

We perform comprehensive assessments to evaluate our fingerprinting scheme. Specifically, drawing on the core idea of the previous cryptography-based watermarking framework for classification models [13], we theoretically prove that our scheme satisfies four important security requirements: *functionality-preserving*, *non-trivial ownership*, *unremovability* and *unforgeability*. Additionally, extensive evaluations over three state-of-the-art GAN models (AttGAN [4], StarGAN [26], STGAN [27]) show that the fingerprints from our methods perform much better than prior strategies in identifying the target GAN models, and maintaining higher robustness against various model and image transformations.

II. PRELIMINARIES

A. Threat Model

We exactly follow the *standard* threat model in prior IP protection works [13]–[20]. The model owner has a valuable GAN model G , e.g., a GAN trained with massive resources. However, the IP of G could be compromised. For instance, “customers who buy a deep learning network might distribute it beyond the terms of the license agreement” [13]; “Adversaries can steal the model (e.g., via malware infection or insider attackers) and sell it on dark net markets” [16]. The goal of the model owner is to detect whether a suspicious model G^s is plagiarized from G . The suspicious model G^s is deployed as an online service (e.g., [9]–[11]), so the model owner has oracle access to it, i.e., he can send arbitrary inputs to G^s and receive the corresponding outputs. The adversary who hosts the plagiarized G^s may alter the model or inference samples. However, such changes must be moderate: (1) They can be performed efficiently with limited computing resources. Otherwise, the adversary loses the motivation of plagiarizing the model. (2) Since the adversary has no knowledge of the verification samples generated by the model owner, the changes

are generally applied to all the inference samples, and cannot affect the model performance over clean samples. The model owner needs a robust solution adaptive to those situations.

B. DNN Fingerprinting

Fingerprinting is a promising technique to protect the IP of deep learning models [17]–[20]. Different from watermarking [13]–[16], the model owner constructs the fingerprint and conducts ownership verification without modifying the target model. This brings much more convenience and applicability. Researchers proposed solutions to fingerprint classification models with adversarial attacks [17]–[20]. The key insight is to craft adversarial examples exclusively for the target model, which assigns unique labels to them. During verification, the model owner uses those samples to query a suspicious model. A matched model will give the desired unique labels as the ownership evidence. An unrelated model will still predict normal ground-truth labels.

It becomes difficult when we migrate these strategies to fingerprinting GANs. The main difference is that the output of a GAN is data samples rather than labels. Using adversarial examples of such models for fingerprinting can lead to two problems. First, the fingerprint is less *persistent*: the output of GANs is more sensitive to model or input transformations than that of classifiers (labels). An adversary can easily remove the fingerprint from the protected model. Second, the fingerprint is less *stealthy*: a unique label from a classification model is still reasonable, as it belongs to one of possible classes. However, a unique data sample from a GAN can be suspicious, and easily recognized by the adversary. We will validate these conclusions in Section VI.

C. Commitments

We adopt the commitment scheme [28] to implement our verification protocol. It is a widely used cryptographic primitive that allows the sender to lock a secret x in a vault that is free of cryptographic information leakage and tamper-proof, and then send it to others (i.e., a receiver). Generally, a commitment scheme contains two algorithms:

- **Com**(x, h): Given a secret $x \in S$ and a random bit string $h \in \{0, 1\}^n$, outputs a bit string c_x , where h transforms x into the ciphertext state. S represents the value space of x .
- **Open**(c_x, x, h): Given a secret $x \in S$, a random bit string $h \in \{0, 1\}^n$, and $c_x \in \{0, 1\}^Z$, if **Com**(x, h) = c_x , outputs 1. Otherwise, outputs 0.

A commitment scheme enjoys the following properties:

Correctness: it is required that for $\forall x \in S$, we have

$$Pr_{h \in \{0,1\}^n} [\text{Open}(c_x, x, h) = 1 | \text{Com}(x, h) \rightarrow c_x] = 1$$

Binding: it is impossible for the sender to change the locked secret x once it is sent out. For any PPT algorithm¹ \mathcal{A} , we have

$$Pr \left[\text{Open}(c_x, \tilde{x}, \tilde{h}) = 1 \mid \begin{array}{l} c_x \leftarrow \text{Com}(x, h) \wedge \\ (\tilde{x}, \tilde{h}) \leftarrow \mathcal{A}(c_x, x, h) \wedge \\ (x, h) \neq (\tilde{x}, \tilde{h}) \end{array} \right] \leq \epsilon(n),$$

¹PPT indicates an algorithm that can be run in probabilistic polynomial time.

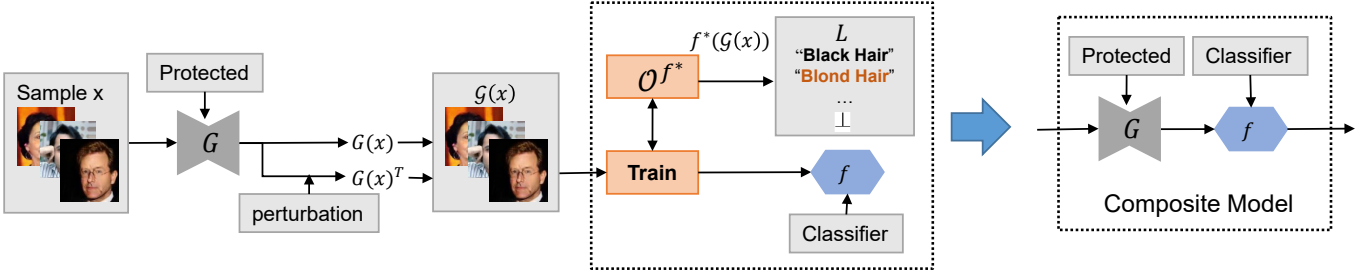


Fig. 2: Training a composite deep learning model.

where $\epsilon(n)$ is negligible in n and the probability is taken over $x \in S$ and $h \in \{0, 1\}^n$.

Hiding: it is infeasible for receivers to open the locked x without the sender's help. It requires that no PPT algorithm \mathcal{A} can distinguish $c_{x'} \leftarrow \mathbf{Com}(x', h)$ from $c_x \leftarrow \mathbf{Com}(x, h)$ for any $x, x' \in S$ and $h \in \{0, 1\}^n$, where $x \neq x'$. If for all $x \neq x'$, the distributions of c_x and $c_{x'}$ are statistically close, i.e., $\Delta(c_x, c_{x'}) = \frac{1}{2} \sum_{c \in \mathcal{Z}} \Pr(c_x = c) - \Pr(c_{x'} = c)$ is a negligible function in n , where \mathcal{Z} denotes the range space of c_x , we call the commitment scheme statistical hiding.

III. A NOVEL FINGERPRINTING SCHEME

A. Design Insight

As discussed above, to make the verification stealthier and more indistinguishable from normal inference, the fingerprint samples and the corresponding model output should be identical to normal cases. Besides, the model output should also be unique to differentiate the target and other unrelated models. Although these two conditions seem to contradict each other, we propose a new scheme to achieve a satisfied tradeoff between them. The general idea is that we craft fingerprint samples with the model output visually similar to normal ones, and employ a classifier to tell if the output is from a target model or not (Fig. 1b). A matched GAN model will produce visually normal output samples, but assigned unique labels by the classifier. Below, we describe the detailed steps of our scheme.

B. Scheme Overview

We consider an image-to-image translation GAN model for IP protection. We introduce an additional classifier for ownership judgement, which forms a *composite deep learning model* with the target GAN. Then we carefully craft fingerprints and embed them into the composite model. This process requires that the embedded fingerprint should be difficult to remove, even if the adversary modifies the GAN model or samples.

We borrow the basic framework from [13], which is a standard theoretical analysis of DNN watermarks. As we focus on GAN fingerprinting without any model modification, we need to modify this framework to adapt to this requirement. Below, we first give the formal definitions of the composite deep learning model and the fingerprint. Based on these, we give the workflow of our scheme. For simplicity, we use $n \in \mathbb{N}$ as a security parameter, which is implicit in the input of all algorithms below. $[k]$ is the shorthand $\{1, 2, \dots, k\}$ for $k \in \mathbb{N}$. The details of all important symbols and notations we use are listed in Appendix A.

C. Composite Deep Learning Model

We consider a target GAN model G for protection², which maps a sample $x \in D$ to another sample $x' \in D$. Here $D \subset \{0, 1\}^*$ is the sample space. We introduce a label space $L \subset \{0, 1\}^* \cup \{\perp\}$ for any sample in D , which defines the possible properties of the samples generated by G , e.g., objects, scenes or conditions in the image. We define $|D| = \Theta(2^n)$ and $|L| = \Omega(p(n))$ for a positive polynomial $p(\cdot)$. A composite deep learning model is defined as below:

Definition 1. (*Composite Deep Learning Model*) Given the GAN model G and its sample space D , let f^* be a ground-truth function which classifies a sample $x \in D$ according to its label $y \in L$. Let $\mathcal{G}(x) = \{G(x) \cup (G(x))^T | x \in D\}$ be the augmented set of model outputs, where $G(x)$ and $(G(x))^T$ denote the accurate model outputs and possible perturbed ones³. We use the **Train** algorithm described below to obtain a classifier f , which approximates the mapping: $\mathcal{G}(x) \rightarrow f^*(\mathcal{G}(x))$. Then a composite deep learning model is defined as $M(x) = f(G(x))$.

The composite model is essentially a mapping $M : D \rightarrow L$, which simulates how humans assign specific labels to GAN-generated samples. To produce the composite model from G and f^* , we consider an oracle \mathcal{O}^{f^*} , which truly answers each call to f^* . Then we have the following algorithms.

- **Train**($\mathcal{O}^{f^*}, \mathcal{G}$): it is a PPT algorithm used to output a classifier $f \subset \{0, 1\}^{p(n)}$, where $p(n)$ is a polynomial in n .
- **Classify**(M, x): it is a deterministic function that outputs a value $M(x) \in L \setminus \{\perp\}$ for a given input $x \in D$.

Fig. 2 gives an example of training a composite deep learning model. We use $\bar{D} = \{x \in D | M(x) \neq \perp\}$ to denote the set of all inputs whose relationship with the output is defined. Then we say the algorithms (**Train**, **Classify**) are ϵ -accurate if $\Pr[f^*(\mathcal{G}(x)) \neq \mathbf{Classify}(M, x) | x \in \bar{D}] \leq \epsilon$, where the probability arises from the randomness of **Train**. Thus, we measure accuracy mainly for those inputs that are meaningful to the outputs. For those inputs not defined by the ground-truth classifier f^* , we assume their labels are random, i.e., for all $x \in D \setminus \bar{D}$ and any $i \in L$, we have $\Pr[\mathbf{Classify}(M, x) = i] = 1/|L|$.

²Here G is only the generator of the GAN model, as the discriminator is deprecated after the GAN is trained.

³ $(G(x))^T$ is used for training to improve the classification accuracy of f even on the (subtle) perturbations of $G(x)$.

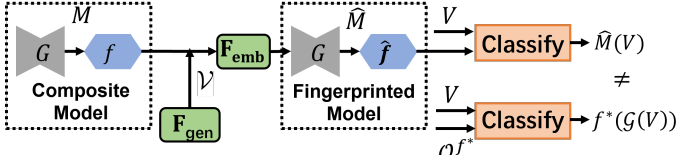


Fig. 3: **Generating a fingerprinted composite model.**

D. Fingerprints in Composite Models

Our fingerprinting scheme crafts a set of verification samples and a classifier, such that the classifier can assign unique labels to the target model’s outputs of these verification samples. Formally, we have the following definition:

Definition 2. (*Fingerprint Set for a Composite Model*) A fingerprint set \mathcal{V} for a composite model M is defined as (V, V_L) , where the verification sample set $V \subset D$ and verification label set $V_L \subset L \setminus \{\perp\}$ satisfy the condition: for $x \in V$, $V_L(x) \neq f^*(G(x))$.

We use an algorithm F_{gen} to generate a fingerprint set⁴ from the GAN model G and oracle \mathcal{O}^{f^*} . We further define a PPT algorithm F_{emb} to embed the generated fingerprint into the composite model. Specifically, given the oracle \mathcal{O}^{f^*} , a fingerprint set \mathcal{V} , and a composite model M , F_{emb} produces a fingerprinted model $\hat{M} = f(G(\cdot))$, which can correctly classify the verification samples V as V_L with a high probability (Fig. 3). Formally, we have the following definition:

Definition 3. (*Fingerprinted Model*) We say a composite model \hat{M} is fingerprinted by F_{emb} , if it behaves like $f^*(G(\cdot))$ on $D \setminus V$, and reliably predicts unique labels V_L on V , i.e.,

$$\begin{aligned} & \Pr_{x \in D \setminus V} [f^*(G(x)) \neq \text{Classify}(\hat{M}, x)] \leq \epsilon, \text{ and} \\ & \Pr_{x \in V} [V_L(x) \neq \text{Classify}(\hat{M}, x)] \leq \epsilon. \end{aligned} \quad (1)$$

Remark: since a given model may be suspected of being embedded with fingerprints, a strong fingerprint should be difficult to be reconstructed or detected by adversaries in arbitrary ways. It requires the fingerprints to satisfy additional requirements to endure various types of attacks. For legibility, we will present these requirements in Section IV-A.

E. Workflow of Our Fingerprinting Scheme

We now outline our fingerprinting process, as shown in Fig. 4. Given the targeted model G , the model owner first adopts the algorithm **Train** to establish the composite deep learning model M . Then he uses a series of algorithms to generate a secret marking key mk and a public verification key vk , and embed the fingerprint from mk into the model. During verification, the model owner uses marking and verification keys to verify whether a suspicious model contains the fingerprints. To be more precise, the entire workflow can be described by three high-level PPT algorithms (**KeyGen**, **FP**, **Verify**):

- **KeyGen**(n): Given a security parameter n and the information related to the model, it outputs the secret marking key

⁴Whenever we fix a verification sample set V , the fingerprint set implies the corresponding V_L .

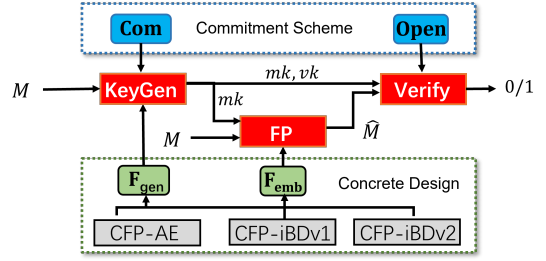


Fig. 4: **The workflow of our fingerprinting scheme.**

mk and the public verification key vk , where mk contains the fingerprint to be embedded into the target model, and vk is used for subsequent verification. This process requires F_{gen} to generate fingerprint sets. It also requires **Com** to commit to the elements in each fingerprint set and random elements selected by the model owner, which provides arguments for subsequent verification.

- **FP**(M, mk): Given a composite model M and the marking key mk , it outputs a fingerprinted model \hat{M} . This process uses F_{emb} as the subroutine to convert M to \hat{M} , thereby embedding the fingerprint contained in mk into M .
- **Verify**(mk, vk, M): Given the key pair mk, vk and a model M , it outputs a bit $b \in \{0, 1\}$, where 1 means that the verified model has copyright infringement, and vice versa. This process uses **Open** as the subroutine to open the previous commitments to all the elements in mk .

Fig. 5 details the algorithms (**KeyGen**, **FP**, **Verify**) for this process. Specifically, let (**Train**, **Classify**) be an ϵ -accurate composite deep learning model, F_{emb} be a strong fingerprinting algorithm and (**Com**, **Open**) be a statistically hiding commitment scheme. (1) **KeyGen** generates strong fingerprints (F_{gen}), which are also used as the secret marking key mk . Then a commitment scheme (**Com**) is used to generate the verification key vk corresponding to mk for the legitimacy verification of suspicious models. (2) **FP** embeds the fingerprints into the composite model (F_{emb}). (3) **Verify** opens the commitments (**Open**) to all the elements in the secret key mk , and uses it to verify whether a suspicious model matches the fingerprints (**Classify**). If most verification samples in the fingerprint set are predicted as the verification labels by the classifier \hat{f} , we infer this GAN model is infringing.

F. Security Requirements

The correctness of our fingerprinting scheme, i.e., three PPT algorithms (**KeyGen**, **FP**, **Verify**), requires that for the honestly generated keys mk, vk , we have

$$\Pr_{(M, \hat{M}, mk, vk)} [\text{Verify}(mk, vk, \hat{M}) = 1] = 1.$$

We now define the following four security requirements:

- (I) **Functionality-preserving.** This property is twofold in our fingerprinting scheme. The model with fingerprints should be as accurate as the model without fingerprints for classifying normal samples. The proposed scheme should also correctly classify the verification samples V as V_L with a high probability. Formally, for any (\hat{M}, mk, vk) honestly generated through the previously described algorithms, it holds that

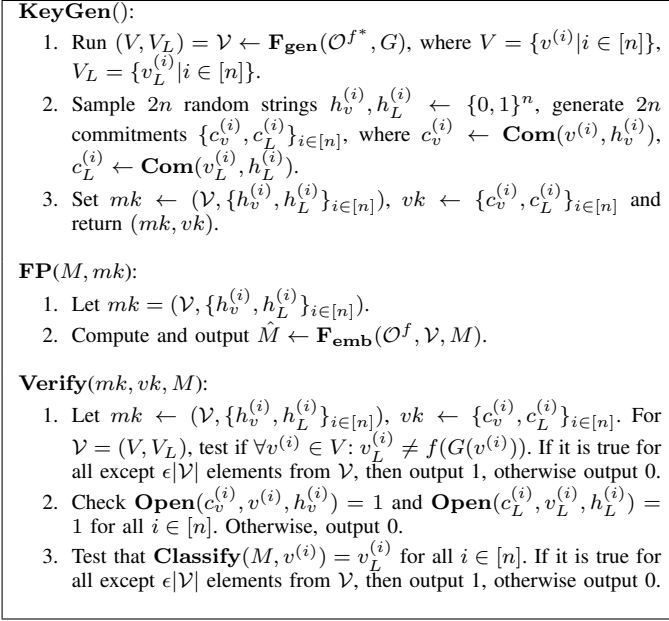


Figure 5: **End-to-end fingerprinting process.**

$$\Pr_{x \in \mathcal{D} \setminus \mathcal{V}} [f^*(G(x)) \neq \mathbf{Classify}(\hat{M}, x)] \leq \epsilon, \text{ and}$$

$$\Pr_{x \in \mathcal{V}} [V_L(x) \neq \mathbf{Classify}(\hat{M}, x)] \leq \epsilon.$$

(II) **Non-trivial ownership.** This property requires that it is impossible for an adversary to construct a key pair (mk, vk) in advance to claim the ownership of an arbitrary model that is unknown to him, even if he knows the fingerprinting algorithm. Formally, a fingerprinting scheme with non-trivial ownership requires that any PPT algorithm \mathcal{A} wins the following **Game 1** only with a negligible probability.

1. Run \mathcal{A} to compute $(\tilde{mk}, \tilde{vk}) \leftarrow \mathcal{A}()$.
2. Generate $M \leftarrow \mathbf{Train}(\mathcal{O}^{f^*}, G)$.
3. Sample $(mk, vk) \leftarrow \mathbf{KeyGen}()$.
4. Compute $\hat{M} \leftarrow \mathbf{FP}(M, mk)$.
5. \mathcal{A} wins if $\mathbf{Verify}(\tilde{mk}, \tilde{vk}, \hat{M}) = 1$.

(III) **Unremovability.** This means that the adversary cannot remove the fingerprint even if he knows its existence and the algorithms used. Formally, a fingerprinting scheme with unremovability requires that any PPT algorithm \mathcal{A} wins the following **Game 2** only with a negligible probability.

1. Generate $M \leftarrow \mathbf{Train}(\mathcal{O}^{f^*}, G)$ and $(mk, vk) \leftarrow \mathbf{KeyGen}()$.
2. Compute $\hat{M} \leftarrow \mathbf{FP}(M, mk)$.
3. Run \mathcal{A} to compute $\tilde{M} \leftarrow \mathcal{A}(\mathcal{O}^f, \hat{M}, vk)$.
4. \mathcal{A} wins if

$$\Pr_{x \in \mathcal{D}} [\mathbf{Classify}(M, x) = f^*(G(x))] \approx$$

$$\Pr_{x \in \mathcal{D}} [\mathbf{Classify}(\tilde{M}, x) = f^*(G(x))] \text{ and } \mathbf{Verify}(mk, vk, \tilde{M}) = 0.$$

(IV) **Unforgeability.** This property requires that even if the adversary knows vk , he cannot convince a third party that he has the property rights to the model without knowing mk . Formally, a fingerprinting scheme with unforgeability requires that any PPT algorithm \mathcal{A} wins the following **Game 3** only with negligible probability.

1. Generate $M \leftarrow \mathbf{Train}(\mathcal{O}^{f^*}, G)$ and $(mk, vk) \leftarrow \mathbf{KeyGen}()$.

2. Compute $\hat{M} \leftarrow \mathbf{FP}(M, mk)$.
3. Run the adversary $(\tilde{mk}, \tilde{M}) \leftarrow \mathcal{A}(\mathcal{O}^f, \hat{M}, vk)$.
4. \mathcal{A} wins if $\mathbf{Verify}(\tilde{mk}, vk, \tilde{M}) = 1$.

IV. CONCRETE METHODOLOGIES OF GENERATING AND EMBEDDING STRONG FINGERPRINTS

A. Assumptions for Strong Fingerprints

With the two algorithms \mathbf{F}_{gen} and \mathbf{F}_{emb} , we expect that the model owner can produce strong fingerprints \mathcal{V} that can exhibit the following three properties. \mathbf{F}_{emb} that takes such samples as input is called a strong fingerprinting algorithm. These are necessary for us to build effective fingerprinting solutions satisfying the requirements in Section III-F.

(1) *Distinctness:* We assume that \mathbf{F}_{gen} can output a fingerprint set of size n each time. To achieve repeatable verification, \mathbf{F}_{gen} is required to iteratively generate fingerprint sets that meet Definition 2. The corresponding fingerprinted model using \mathbf{F}_{emb} need to meet Definition 3. Moreover, a strong fingerprint should satisfy that for any two fingerprint sets generated by \mathbf{F}_{gen} , their verification sample sets V and V' are almost never intersected, i.e., the probability of $\Pr[V \cap V' \neq \emptyset]$ for $(V, V_L), (V', V'_L) \leftarrow \mathbf{F}_{\text{gen}}()$ is negligible in n .

(2) *Stealthiness:* Each verification sample during inference should be indistinguishable from the normal ones, making it difficult for the adversary to respond adaptively and ensuring the concealment of verification. This means that for each verification sample $v^{(i)} \in V$ generated from a randomly selected clean sample $x^{(i)}$, the following expression:

$$\mathcal{H} = \|v^{(i)}, x^{(i)}\| + \|G(v^{(i)}), G(x^{(i)})\| + \sum_j \|G_{v^{(i)}, j}, G_{x^{(i)}, j}\|$$

is minimized, where $G_{v^{(i)}, j}$ and $G_{x^{(i)}, j}$ are the j -th feature maps in G , and $\|\cdot, \cdot\|$ is a distance function⁵.

(3) *Persistency:* \mathbf{F}_{emb} is able to embed the fingerprint persistently such that the adversary cannot revert the fingerprinted model back to the original one. This property is discussed under two assumptions. First, the adversary has limited computing resources, which do not support him to retrain a clean model from scratch. Otherwise, he will lose the motivation of stealing others' models. Second, the adversary is not willing to erase the fingerprint at the cost of huge accuracy drop for the plagiarized model. Hence, we define the persistency as follows: let \mathcal{O}^{f^*} be a ground-truth oracle, \mathcal{V} be a fingerprint set, and $\hat{M} \leftarrow \mathbf{F}_{\text{emb}}(\mathcal{O}^{f^*}, \mathcal{V}, M)$ be a ϵ -accurate model. Assume an algorithm \mathcal{A} on input \mathcal{O}^{f^*} , \hat{M} outputs a model \tilde{M} in polynomial time t which is at least $(1-\epsilon)$ accurate on \mathcal{V} . Then, for any arbitrary model N , $\tilde{N} \leftarrow \mathbf{F}_{\text{emb}}(\mathcal{O}^{f^*}, N)$ generated in same time t , is also ϵ -accurate.

Below we present three novel concrete designs based on our fingerprinting scheme. For each design, we describe the two crucial algorithms \mathbf{F}_{gen} and \mathbf{F}_{emb} for generating strong fingerprints and embedding them into the model, respectively.

⁵Note that the stealthiness of fingerprints is difficult to describe with cryptographic primitives, because it is very subjective. We mainly demonstrate the superiority of the generated fingerprint based on empirical experiments.

B. CFP-AE

Our first method, CFP-AE (Composite Fingerprint based on Adversarial Examples), is inspired by the generative adversarial examples [29]. Different from the traditional fingerprinting methods [17], [18] that directly craft adversarial examples against the target model, we propose to make the target GAN model generate adversarial examples to the classifier. The output sample of the target model looks normal, while the output label of the classifier is unique as the ownership evidence.

Algorithm 1 shows the detailed process of generating the fingerprint set. Given \mathcal{O}^{f^*} , We first train a classifier f for classifying the attributes of the data samples. Then we uniformly select some random samples $\{x^{(i)} | i \in [n]\}$ from the sample space D . Since the size of the space is $\Theta(2^n)$, a PPT adversary only has a negligible probability to infer these samples. We craft the verification samples $v^{(i)}$ from these clean samples using an optimization method. To ensure the indistinguishability between the verification sample and its corresponding clean sample, for each $v^{(i)}$, we need to minimize $\mathcal{H} = \|v^{(i)}, x^{(i)}\| + \|G(v^{(i)}), G(x^{(i)})\| + \sum_j \|G_{v^{(i)},j}, G_{x^{(i)},j}\|$. Also, a qualified verification sample $v^{(i)}$ should enable the classifier to maximize the distance between the ground-truth label $y^{(i)}$ corresponding to $G(x^{(i)})$ and predicted label $f(G(v^{(i)}))$. To achieve these, we construct a loss function $F_{obj}(\mathcal{O}^f, G, \{x^{(i)}, y^{(i)}\}, v^{(i)})$ as follows.

$$F_{obj}(\mathcal{O}^f, G, \{x^{(i)}, y^{(i)}\}, v^{(i)}) = \sum_c y_c^{(i)} \log(f(G(v^{(i)}))_c) + \sum (v^{(i)} - x^{(i)})^2 + \sum (G(v^{(i)}) - G(x^{(i)}))^2 + \sum_j \sum (G_{v^{(i)},j} - G_{x^{(i)},j})^2, \quad (2)$$

where $G_{v^{(i)},j}$ and $G_{x^{(i)},j}$ are the j -th feature maps in G when processing $v^{(i)}$ and $x^{(i)}$, respectively. We iteratively search for the optimal $v^{(i)}$ by minimizing the above objective function. As a result, we obtain the final verification sample $v^{(i)}$ with the label $f(G(v^{(i)})) = v_L^{(i)} \neq f^*(G(v^{(i)}))$.

Algorithm 1: Fingerprint Generation

- F_{gen}** (\mathcal{O}^{f^*}, G)
- 1: Train a normal classifier f with \mathcal{O}^{f^*} and target GAN model G .
 - 2: Uniformly select random samples $\{x, y\} \in D$ n times to build $X = \{x^{(1)}, \dots, x^{(n)}\}$ and $Y = \{y^{(1)}, \dots, y^{(n)}\}$.
 - 3: **for** each $\{x^{(i)}, y^{(i)}\} \in \{X, Y\}$ **do**
 - 4: Generate $v^{(i)}$ from $\{x^{(i)}, y^{(i)}\}$ by minimizing the objective function $F_{obj}(\mathcal{O}^f, G, \{x^{(i)}, y^{(i)}\}, v^{(i)})$ in Equation 2.
 - 5: Generate $\{v_L^{(i)} | i \in [n]\}$ with label $v_L^{(i)} = f(G(v^{(i)})) \neq f^*(G(v^{(i)}))$.
 - 6: **end for**
 - 7: **Return** a fingerprint $\mathcal{V} = (V, V_L)$, where $V = \{v^{(i)} | i \in [n]\}$ and $V_L = \{v_L^{(i)} | i \in [n]\}$.
-

It is worth noting that in CFP-AE, we do not need to modify the classifier f after we perform the **F_{gen}** function. We can directly use the generated samples to query the composite model for ownership verification. Hence, the **F_{emb}** function is empty with $\hat{f} = f$ in this method.

C. CFP-iBDv1

Our second method, CFP-iBDv1 (Composite Fingerprint based on invisible Backdoor (version 1)), utilizes the invisible backdoor attack technique [22]. The key idea is to make the target model produce output samples containing invisible triggers, which will activate the backdoor embedded in the classifier to predict unique labels. CFP-iBDv1 requires two steps. Fingerprint generation calls the same function **F_{gen}** as in CFP-AE to produce verification samples and labels. Then we perform the fingerprint embedding **F_{emb}**($\mathcal{O}^f, \mathcal{V}, M$), which further fine-tunes the classifier f into \hat{f} , to better recognize the relationships between the verification samples and labels.

Algorithm 2 shows the detailed process of fine-tuning the classifier. We prepare two sets: the verification set $\mathcal{V}_s = (G(V), V_L)$, where V and V_L are generated from **F_{gen}**; the normal set $\mathcal{N}_s = (G(X), Y)$, where X contains samples generating V in **F_{gen}** and Y contains labels corresponding to samples in $G(X)$. Since the fingerprint must be persistent against image transformations, we further perform data augmentation over these two sets with common transformation functions. Using these two augmented sets \mathcal{V}_s^a and \mathcal{N}_s^a , we fine-tune the classifier as \hat{f} , and finally obtain the composite model $\hat{M}(\cdot) = \hat{f}(G(\cdot))$.

Algorithm 2: Fingerprint Embedding

- F_{emb}**($\mathcal{O}^f, \mathcal{V}, M$)
- 1: $(V, V_L) = \mathcal{V}$.
 - 2: $\mathcal{V}_s = (G(V), V_L)$.
 - 3: $\mathcal{N}_s = (G(X), Y)$, X and Y are from **F_{gen}**.
 - 4: Augment these two sets to obtain \mathcal{V}_s^a and \mathcal{N}_s^a .
 - 5: Fine-tune f into \hat{f} with \mathcal{V}_s^a and \mathcal{N}_s^a together by minimizing the loss function \mathcal{L}_{ft} .
 - 6: **Return** fingerprinted model $\hat{M}(\cdot) = \hat{f}(G(\cdot))$.
-

We use the cross-entropy loss function to fine-tune the classifier with the two sets:

$$\mathcal{L}_{ft} = \mathcal{L}_{G1}(\mathcal{O}^f, \mathcal{V}_s^a, \mathcal{N}_s^a) = - \sum_{(x,y) \in \mathcal{V}_s^a} \sum_c y_c \log(f(x)_c) - \sum_{(x,y) \in \mathcal{N}_s^a} \sum_c y_c \log(f(x)_c),$$

where c is the label index of f .

D. CFP-iBDv2

Our third method, CFP-iBDv2 (Composite Fingerprint based on invisible Backdoor (version 2)), is an advanced version of CFP-iBDv1. We follow the same algorithms to generate fingerprints and embed them into the model. A novel loss function is introduced to fine-tune the classifier for better robustness and effectiveness.

First, we adopt the idea of the Triplet Loss [23] to enhance the persistency of our fingerprints. The Triplet Loss is able to distinguish different objects under similar conditions (e.g., pose, illumination). It achieves this by minimizing the inner representation (i.e., feature embedding) difference of the same object with different external conditions, while maximizing the difference of different objects with the same condition.

Similarly, we can minimize the distance of different verification samples in the feature space, and maximize the distance of a verification and normal samples. This can increase the probability that the fine-tuned classifier will give unique labels for verification samples. The loss function is as below:

$$\mathcal{L}_{G2}(\mathcal{M}, \mathcal{V}_s^a, \mathcal{N}_s^a, m) = \sum_{v_a \in \mathcal{V}_s^a} \max\{\max_{v_p \in \mathcal{V}_s^a} (\sum (\mathcal{M}(v_a) - \mathcal{M}(v_p))^2) - \min_{x \in \mathcal{N}_s^a} (\sum (\mathcal{M}(v_a) - \mathcal{M}(x))^2) + m, 0\},$$

where m is a constant, and $\mathcal{M}(\cdot)$ represents the feature embedding in the feature space before the classification layers.

Second, we apply the fine-grained categorization approaches [24], [25] to fine-tune the classifier. Fine-grained categorization aims to classify an object into an exact sub-category, e.g., the brand of a car, the species of a bird. Various techniques have been introduced to achieve this challenging goal [30]–[32]. We can treat the fingerprint embedding process as a fine-grained categorization task, where samples from \mathcal{V}_s^a are in one category (fingerprint verification), while samples from \mathcal{N}_s^a are in another category (normal inference). Specifically, we change the classifier to a multitask one: the original network is used to predict the attribute, while a new classification layer is added to predict the verification category (label “1” for fingerprint verification; label “0” for normal inference). Then we adopt the Entropy-Confusion Loss [33] to train the multi-task model:

$$\mathcal{L}_{G3}(\mathcal{B}, \mathcal{V}_s^a, \mathcal{N}_s^a, \epsilon) = \sum_{v \in \mathcal{V}_s^a} (\mathcal{B}(v)_0 \log \frac{\mathcal{B}(v)_0}{\mathcal{B}(v)_1 + \epsilon} + (\mathcal{B}(v)_1 + 1) \log \mathcal{B}(v)_1) + \sum_{x \in \mathcal{N}_s^a} ((\mathcal{B}(x)_0 + 1) \log \mathcal{B}(x)_0 + \mathcal{B}(x)_1 \log \frac{\mathcal{B}(x)_1}{\mathcal{B}(v)_0 + \epsilon}),$$

where $\epsilon = 1e^{-5}$ is a constant to avoid a denominator of zero, $\mathcal{B}(\cdot)$ is the output from the added binary classification layer, and $\mathcal{B}(\cdot)_i$ is the i -th element in the output. Hence, our ultimate loss function \mathcal{L}_{ft} used to fine-tune f is

$$\mathcal{L}_{ft} = \mathcal{L}_{G1} + \mathcal{L}_{G2} + \mathcal{L}_{G3}.$$

After we finish the classifier fine-tuning, we remove the binary classification layer from \hat{f} , and integrate it with the target GAN model to form the composite model \hat{M} .

V. SECURITY ANALYSIS

Assuming \mathbf{F}_{emb} is a strong fingerprinting algorithm that can generate fingerprints with the three properties in Section IV-A, we prove our fingerprinting scheme can satisfy the four requirements in Section III-F.

Theorem 1. *Let \bar{D} be of super-polynomial size in n . Given the commitment scheme and the strong fingerprinting algorithm, the algorithms (**KeyGen**, **FP**, **Verify**) in Fig. 5 form a privately verifiable fingerprinting scheme, which satisfies the requirements of functionality-preserving, non-trivial ownership, unremovability, and unforgeability.*

Proof (Sketch): Our proof relies on the security of the commitment scheme and assumptions of strong fingerprints. In

detail, the *hiding* property of the commitment scheme enables the public verification key to hide useful information about the fingerprint from the adversary (i.e., unforgeability), while the *binding* property ensures that one cannot claim the ownership of a model from others (i.e., non-trivial ownership). Also, as defined in Section IV-A, a strong fingerprint embedded into the model should (i) be distinctive, i.e., behaves like $f^*(\mathcal{G}(\cdot))$ on $\bar{D} \setminus V$ and reliably predicts unique labels V_L on V (i.e., functionality-preserving), and (ii) be persistent such that the adversary cannot revert the fingerprinted model back to the original one in time t (i.e., unremovability). Based on these, we can prove that our designs satisfy the above requirements. For the technical details of the proof, please see Appendix C.

Remark: The algorithm **Verify** only allows verification by honest parties in a private way, since mk will be known once **Verify** is run, which allows the adversary to retrain the model on the verification sample set. It is not a problem for the applications such as IP protection, because there are trusted third parties in the form of judges. However, for practicality, we may still hope to design a publicly verifiable method without limiting the number of repeated verifications. To achieve this, we can use a powerful cryptographic primitive called the *zero-knowledge proof argument* [34], to convert our fingerprinting scheme from private verifiability to public verifiability. For more details, please refer to Appendix D.

VI. EXPERIMENTS

We conduct comprehensive experiments to validate that our concrete designs can meet the strong fingerprint requirements in Section IV-A. We report the main results, and a plethora of experimental results can be found in Appendix G-B.

Model and dataset. Our scheme can be applied to general image-to-image translation GAN models and tasks, since the design does not rely on any assumptions about datasets, model architectures or parameters. Without loss of generality, we employ three mainstream GANs (i.e., AttGAN [4], StarGAN [26], and STGAN [27]) for evaluations, all of which take a face image as input, and produce an image with modified attributes specified by the user. We train each model to edit five attributes: (A1) black hair, (A2) blond hair, (A3) brown hair, (A4) male and (A5) young. We adopt a public dataset CelebA [35], which is a standard benchmark dataset used in this area.

Scheme implementation. In our experiments, the property classifier f is implemented by ResNet34 [36]. We train f as a multi-label classifier on the CelebA dataset to predict the facial attributes. Each sample in CelebA has 40 annotated attributes. Then the output of f is a 40-bit vector, with each bit representing whether the image has the corresponding attribute. Note that the construction of f is general, so other mainstream classification models can be applied to our task. We compare the time cost of training a GAN and generating verification samples for it in Appendix H.

For \mathbf{F}_{gen} in Algorithm 1, we select 100 random samples from CelebA as the verification sample set V . For each sample, we set its unique verification label $V_L(x)$ by flipping each bit in its ground-truth label vector. We minimize F_{obj} in

Equation 2 under the constraint $\|G(v^{(i)}), G(x^{(i)})\| \leq \delta$. We set $\delta = 9e^{-4}$, which is proven to be sufficient to ensure the indistinguishability between the verification sample and its corresponding clean sample. The generated verification sample set can be used for all the three proposed methods. After V is crafted, we keep all the flipped 40 attributes as the verification label for CFP-iBDv1 and CFP-iBDv2. For CFP-AE, we only flip 5 attributes, while the rest attributes are the same as the ground truth. These attributes are selected as the easiest ones to be misclassified by analyzing the decision boundary of the classifier. They are listed in Appendix E.

For CFP-AE, we do not need to make any changes to the classifier f . For CFP-iBDv1 and CFP-iBDv2, we need to embed the fingerprint into the composite model following \mathbf{F}_{emb} in Algorithm 2. We fix \mathcal{G} , while fine-tuning the classifier f using the prepared verification sample set. This will give us the final fingerprint-embedded composite model $\hat{M} = \hat{f}(G(\cdot))$. For \mathbf{F}_{emb} in Algorithm 2, to enhance the robustness of the fingerprinted classifier, we adopt four types of mainstream image transformations (adding noise, blurring, compression and cropping) to augment the verification sample set \mathcal{V}_s and normal sample set \mathcal{N}_s . We fine-tune f with only 100 verification samples and 100 normal samples, so it is very efficient for the model owner to annotate these samples.

For verification, we query the suspicious GAN model with 100 verification samples. Similar to prior works [14], [15], [17], [18], [20], we empirically set the threshold τ for ownership judgement, which is 0.8.

Baselines. Since there are no existing works for fingerprinting image-to-image translation GAN models, we migrate the fingerprinting strategy from classification models to GANs as our baselines. Past works proposed two types of common techniques to generate adversarial attacks for GAN models, which are adopted for fingerprint generation in our baselines. Specifically, (1) AE-D leverages the *distortion attack* [37]–[41], whose outputs are distorted away from the correct one. This is achieved by maximizing the distance between the adversarial output and ground-truth output. During verification, we determine the legitimacy of the suspicious model by measuring the noise ratio of the responses and ground-truth outputs. A model is considered as illegal if the peak signal-to-noise ratio (PSNR) [42] is smaller than a threshold (20). (2) AE-I leverages the *identity attack* [40], [41], whose outputs are identical with the inputs. This is achieved by minimizing the distance between the sample outputs and inputs. During verification, we measure the similarity between the verification samples and the corresponding responses. We flag the model as pirated if their Euclidean distance is smaller than a threshold ($9e^{-4}$). Both types of adversarial examples are generated by C&W [43], which is also used in [17] for fingerprinting classification models.

Metrics. We introduce two metrics: (1) Match Score for Verification samples (MSV) denotes the match ratio of verification labels for verification samples; (2) Match Score for Clean samples (MSC) denotes the match ratio of ground-truth labels for clean samples. For a good fingerprinting method, the target model should have high MSV and MSC, while the MSV on

unrelated models should be low.

A. Distinctness Analysis

Table 1: **MSC (%) and MSV (%) for verifying different GAN models.** \downarrow means a lower score is better. \uparrow means a higher score is better. Same for the following tables.

GAN Structure	Method	Target GAN		Non-target GAN		
		MSC \uparrow	MSV \uparrow	StarGAN	AttGAN	STGAN
				MSV \downarrow	MSV \downarrow	MSV \downarrow
StarGAN	AE-I	100.00	100.00	0.00	0.00	0.00
	AE-D	100.00	100.00	100.00	20.00	12.00
	CFP-AE	100.00	100.00	50.20	33.80	30.40
	CFP-iBDv1	95.52	94.12	62.10	15.10	27.00
	CFP-iBDv2	92.87	90.05	39.62	12.53	16.92
AttGAN	AE-I	100.00	100.00	0.00	0.00	0.00
	AE-D	100.00	14.00	35.00	1.00	6.00
	CFP-AE	100.00	100.00	29.00	42.20	39.80
	CFP-iBDv1	93.40	92.45	49.10	34.20	57.02
	CFP-iBDv2	91.03	90.70	27.15	17.85	30.10
STGAN	AE-I	98.00	100.00	0.00	0.00	13.00
	AE-D	100.00	34.00	66.00	22.00	1.00
	CFP-AE	100.00	100.00	26.20	25.80	67.80
	CFP-iBDv1	93.53	91.57	50.52	42.08	83.20
	CFP-iBDv2	92.20	90.18	30.05	28.75	69.05

We show that the generated verification samples can exclusively identify the target GAN models. We generate verification samples and fingerprinted classifier from one target GAN model, and use them to verify the model itself, as well as other unrelated GAN models, including a model trained with the same configurations (network structure, algorithm, hyperparameters and dataset). Table 1 presents the Match Scores for different models. We observe that all methods perform well on the target model. For other unrelated models, AE-I performs the best in reducing the false positives. This indicates the adversarial identity attack has much lower transferability to other models. We will show that AE-I is impractical in terms of persistency (Section VI-B). AE-D has high transferability for StarGAN, hence it fails to distinguish target and non-target GAN models trained from the same StarGAN. Our methods are generally fair to distinguish target and non-target models with a threshold $\tau = 0.8$. CFP-iBDv2 is better than CFP-AE and CFP-iBDv1, due to the utilization of more sophisticated loss functions when fine-tuning the classifier. We find the results on STGAN are worse than other GANs. The reason is that STGAN has worse performance on facial editing tasks, which can be found in Appendix F. Therefore, for high-quality GANs for commercial use, our scheme can successfully protect their IPs.

B. Persistency Analysis

We adopt the mainstream operations in prior watermarking or fingerprinting works [13]–[20] to evaluate the persistency of different fingerprinting methods.

Persistency against model transformations. We apply pruning and fine-tuning⁶ to moderately alter the GAN model. We also tried model quantification, which could significantly decrease the model usability [44] (see Appendix G-B). So we

⁶Fine-tuning GANs is actually not practical for an adversary to perform, as it requires the discriminator, which is kept secret by the model owner (see Appendix B). To demonstrate the strong persistency of our method, we still evaluate this impractical attack.

Table 2: MSC (%) and MSV (%) after two model transformations.

GAN Structure	Method	Target GAN		Fine-tuning (epochs)						Pruning (compression ratio)			
				10		20		30		0.2		0.4	
		MSC \uparrow	MSV \uparrow	MSC \uparrow	MSV \uparrow	MSC \uparrow	MSV \uparrow	MSC \uparrow	MSV \uparrow	MSC \uparrow	MSV \uparrow	MSC \uparrow	MSV \uparrow
StarGAN	AE-I	100.00	100.00	100.00	0.00	100.00	6.00	100.00	2.00	100.00	43.00	100.00	0.00
	AE-D	100.00	100.00	100.00	100.00	99.00	100.00	100.00	100.00	100.00	100.00	100.00	100.00
	CFP-AE	100.00	100.00	96.60	94.20	96.40	91.80	97.00	96.00	98.80	98.20	94.60	97.00
	CFP-iBDv1	95.52	94.12	94.98	93.07	92.20	89.25	92.88	92.15	95.58	94.12	95.35	93.60
	CFP-iBDv2	92.87	90.05	92.53	85.32	92.28	84.57	92.68	84.80	92.73	90.02	92.78	89.57
AttGAN	AE-I	100.00	100.00	100.00	91.00	100.00	84.00	100.00	75.00	100.00	22.00	100.00	0.00
	AE-D	100.00	14.00	100.00	14.00	100.00	14.00	100.00	14.00	100.00	14.00	100.00	16.00
	CFP-AE	100.00	100.00	98.60	94.60	99.80	95.40	99.00	94.80	97.80	91.20	86.40	87.40
	CFP-iBDv1	93.40	92.45	93.33	92.37	93.45	92.40	93.45	92.37	93.53	92.40	93.08	89.00
	CFP-iBDv2	91.03	90.70	91.93	90.62	92.00	90.70	92.05	90.67	91.98	90.75	91.95	84.95
STGAN	AE-I	98.00	100.00	100.00	85.00	99.00	75.00	92.00	73.00	100.00	58.00	100.00	0.00
	AE-D	100.00	34.00	100.00	36.00	100.00	36.00	100.00	32.00	100.00	34.00	100.00	57.00
	CFP-AE	100.00	100.00	99.40	95.40	99.80	95.20	99.40	94.60	98.60	95.00	93.40	86.60
	CFP-iBDv1	93.53	91.57	93.58	91.62	93.53	91.72	93.28	91.80	93.38	91.45	84.20	91.40
	CFP-iBDv2	92.20	90.18	92.08	90.30	92.20	90.25	91.95	90.40	91.55	90.22	88.98	83.35

Table 3: MSC (%) and MSV (%) after four image transformations.

GAN Structure	Method	Target GAN		Image Transformation									
				Noise		Blur		Compression		Crop			
		MSC \uparrow	MSV \uparrow	MSC \uparrow	MSV \uparrow	MSC \uparrow	MSV \uparrow	MSC \uparrow	MSV \uparrow	MSC \uparrow	MSV \uparrow		
StarGAN	AE-I	100.00	100.00	100.00	1.00	100.00	0.00	100.00	0.00	100.00	0.00	100.00	0.00
	AE-D	100.00	100.00	100.00	100.00	100.00	100.00	100.00	100.00	3.00	100.00	100.00	100.00
	CFP-AE	100.00	100.00	67.20	77.60	83.20	84.60	89.20	89.00	80.00	81.60	80.00	81.60
	CFP-iBDv1	95.52	94.12	94.75	93.12	94.85	93.57	95.03	93.75	95.03	93.57	95.03	93.57
	CFP-iBDv2	92.87	90.05	92.83	86.02	92.05	87.57	92.30	89.70	92.25	90.62	92.25	90.62
AttGAN	AE-I	100.00	100.00	100.00	1.00	100.00	0.00	100.00	0.00	100.00	0.00	100.00	0.00
	AE-D	100.00	14.00	100.00	18.00	100.00	14.00	100.00	14.00	4.00	97.00	100.00	97.00
	CFP-AE	100.00	100.00	67.20	82.00	80.20	73.00	86.80	84.80	67.60	76.80	67.60	76.80
	CFP-iBDv1	93.40	92.45	92.60	91.20	92.75	92.07	92.90	92.52	93.33	91.57	93.33	91.57
	CFP-iBDv2	91.03	90.70	91.38	80.32	91.40	84.10	91.58	89.30	91.58	88.82	91.58	88.82
STGAN	AE-I	98.00	100.00	100.00	0.00	100.00	0.00	100.00	0.00	100.00	0.00	100.00	0.00
	AE-D	100.00	34.00	100.00	41.00	100.00	39.00	100.00	36.00	2.00	100.00	100.00	100.00
	CFP-AE	100.00	100.00	85.50	77.00	94.80	41.20	96.00	65.20	84.20	57.00	84.20	57.00
	CFP-iBDv1	93.53	91.57	92.53	89.00	92.98	90.72	93.30	91.45	93.48	90.95	93.48	90.95
	CFP-iBDv2	92.20	90.18	91.53	86.40	91.48	86.55	91.75	88.15	91.58	88.80	91.58	88.80

ignore such operation. (1) For model fine-tuning, we refine the model with different epochs (10, 20 and 30) using the same training set⁷. Such a setting is commonly used in previous works, and also in line with the adversary’s capability in this paper. The learning rate is different for fine-tuning different model structures to avoid the collapse: $9.99e^{-5}$ for StarGAN, $1e^{-4}$ for AttGAN, $2e^{-5}$ for STGAN, which all follow the learning rate adjustment in the original papers. (2) For model pruning, we consider two compression ratios (0.2 and 0.4). Experiments show that a compression ratio higher than 0.4 can cause significant accuracy degradation for GAN models (see Appendix G-B).

As shown in Table 2, AE-I can hardly resist these transformations. This is because the above attacks fundamentally change the generation details of the target model, while the effectiveness of AE-I highly depends on the invariance of these details. AE-D will benefit from these model operations, which can further distort the model output and decrease the PSNR value. But this is still not enough for verifying AttGAN and STGAN. In contrast, our methods achieve satisfactory persistency under these modifications.

Persistency against image transformations. We evaluate the impact of image transformations. We first tried to transform the model input, which significantly degrades the quality of output images and is impractical for the adversary (see

Appendix G-B). So we mainly consider the transformation of model output. We adopt four popular operations: *adding Gaussian noises* (with mean $\mu = 0$ and standard deviation $\sigma = 0.1$), *Gaussian blurring* (with a kernel size of 5), *JPEG compression* (with a compression ratio of 35%), and *center cropping* (from 128×128 to 100×100). These transformations will still maintain the quality of the images. Table 3 reports the Match scores. We observe AE-I is not robust at all, as these operations can significantly compromise the details of the images and invalidate the verification process. For our approach, CFP-AE is less effective for STGAN models. This is because the output of STGAN is more sensitive than other models, due to its adaptive selection structure, which gives more details in the output. In contrast, CFP-iBDv1 and CFP-iBDv2 perform the best, as the backdoor classifier together with the invisible backdoor samples are more robust against these operations, further enhanced by the data augmentation during fingerprint embedding. We also measure the impacts of different transformation strengths and other types of transformation operations in Appendix G-B, which has similar conclusions.

C. Stealthiness Analysis

We assess the stealthiness property from three perspectives. Note that all our three methods share the same verification samples since they use the same \mathbf{F}_{gen} . So we use CFP-* to denote any of our methods.

Sample space indistinguishability. Fig. 6 visually compares the verification query-response images with the ground-truth

⁷Fine-tuning a GAN using a different dataset of the same distribution will give the same conclusion. Fine-tuning using a dataset of different distributions is a challenging task in computer vision, and there are no satisfactory methods for us to follow.

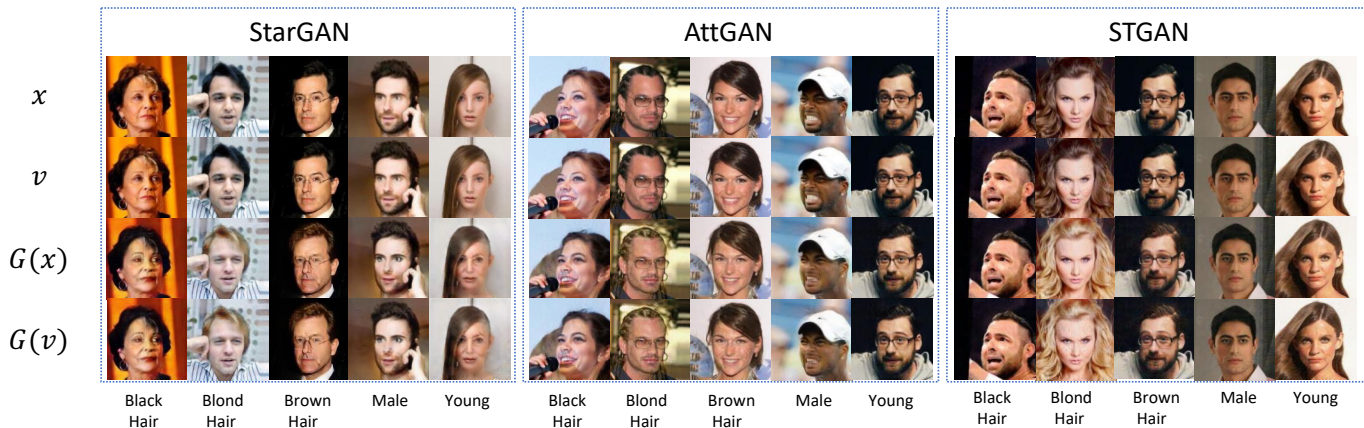


Fig. 6: **Fingerprint visualization.** (a) Clean sample x ; (b) Verification sample v ; (c) GAN output of clean sample $G(x)$; (d) GAN output of verification sample $G(v)$. If the input agrees with the modifying attribute’s label, the model will flip this label and modify the input with the flipped label.

Table 4: **PSNR and SSIM of the verification and clean input (v, x) and output ($G(v), G(x)$) images for different edited attributes.** (“-” in AE-D indicates we are not able to find the qualified verification samples using the algorithm F_{gen} .)

Similarity		StarGAN					AttGAN					STGAN				
		A1	A2	A3	A4	A5	A1	A2	A3	A4	A5	A1	A2	A3	A4	A5
PSNR(v, x)	AE-I	43.84	43.73	43.64	43.72	43.99	39.92	38.68	38.65	39.60	40.07	38.27	38.23	39.50	39.73	39.36
	AE-D	33.62	33.67	33.68	33.57	-	33.70	33.72	33.62	34.09	34.24	33.35	33.81	33.67	-	33.39
	CFP-*	41.54	42.38	42.34	41.12	40.86	47.50	45.54	46.41	46.16	46.41	46.22	44.08	43.48	44.56	44.64
SSIM(v, x)	AE-I	0.99	0.99	0.99	0.99	0.99	0.96	0.95	0.95	0.96	0.96	0.97	0.97	0.98	0.97	0.98
	AE-D	0.89	0.89	0.89	0.89	-	0.90	0.90	0.90	0.91	0.90	0.90	0.90	0.91	-	0.94
	CFP-*	0.98	0.98	0.98	0.98	0.98	0.99	0.99	0.99	0.99	0.99	0.99	0.99	0.99	0.99	0.99
PSNR($G(v), G(x)$)	AE-I	22.44	18.28	23.37	24.59	23.98	30.83	27.79	29.04	29.43	29.66	31.78	33.82	36.32	37.29	36.87
	AE-D	10.99	10.07	10.85	10.77	-	23.94	22.92	24.51	25.65	28.29	22.50	20.12	25.71	-	29.62
	CFP-*	37.75	38.00	38.12	37.37	37.20	45.33	43.33	44.38	44.46	44.36	44.53	42.78	42.81	43.94	44.01
SSIM($G(v), G(x)$)	AE-I	0.84	0.79	0.87	0.87	0.85	0.95	0.92	0.92	0.94	0.94	0.96	0.97	0.98	0.98	0.98
	AE-D	0.40	0.38	0.41	0.40	-	0.86	0.85	0.87	0.89	0.90	0.85	0.84	0.90	-	0.93
	CFP-*	0.97	0.97	0.97	0.96	0.96	0.99	0.99	0.99	0.99	0.99	0.99	0.99	0.99	0.99	0.99

(normal images) for three different GANs using our proposed CFP-*. Visualizations of CFP-* for other GANs, and AE-I and AE-D can be found in Appendix F. We observe that the perturbations added to the verification samples and model output samples are imperceptible. This confirms the effectiveness of the objective function in Equation 2.

Quantitatively, Table 4 shows the peak signal-to-noise ratio (PSNR) and structural similarity (SSIM) [42] between the input of clean and verification samples, as well as between their output samples. According to [45], [46], two pictures with $PSNR > 35$ or $SSIM > 0.95$ can be considered as the same in human vision. We observe that although AE-I and AE-D have indistinguishability for the input samples, their output images are significantly different from ground-truth ones. In contrast, our verification samples meet the visual indistinguishability from normal samples for both model inputs and outputs. This improves the concealment of ownership verification and makes it difficult for adversaries to distinguish verification samples from visual changes.

Feature space indistinguishability. An adversary may try to monitor the intermediate results (e.g., feature maps) of the inference process to detect the verification samples. Anomalous samples usually result in unique behaviors in the feature space, which has been exploited to detect adversarial attacks [47]–[49]. Specifically, we produce 100 samples for each category (normal, AE-I, AE-D, and CFP-*). We compute

Table 5: **The cumulative probability of the standard deviation of feature maps for different types of samples.**

Method	Standard deviation of feature maps							
	0.650	0.675	0.700	0.725	0.750	0.775	0.800	0.825
Normal	0%	3%	9%	15%	38%	63%	92%	100%
AE-I	0%	2%	19%	58%	97%	100%	100%	100%
AE-D	0%	18%	64%	99%	100%	100%	100%	100%
CFP-*	0%	3%	14%	37%	69%	86%	98%	100%

the standard deviation of feature maps for each sample, and then the cumulative probabilities among these 100 samples in one category. If the cumulative probability distribution of one category is closer to that of normal samples, it is harder for the adversary to identify such verification samples in the feature space. Table 5 shows the statistical results. Obviously, the stealthiness of the verification samples from CFP-* is much better than that of AE-I and AE-D since its distribution is closer to the normal one’s. This is because the construction of our verification samples is forced to minimize the distance $\|G_{v,j}, G_{x,j}\|$, which fundamentally ensures the consistency of the distribution in the feature space between verification and normal samples.

Indistinguishability from machine learning detectors. An adversary can employ an anomaly detector to identify verification samples. To show this feasibility, we introduce two detecting scenarios for an adversary. **Scenario 1:** The de-

Table 6: AUC for detecting verification samples.

Method	Scenario 1			Scenario 2		
	l_2	l_1	l_∞	l_2	l_1	l_∞
AE-D	85.74	99.82	86.39	55.46	65.78	55.85
AE-I	75.96	80.37	-	48.19	52.69	-
CFP-*	59.00	-	-	51.51	-	-

tection model accepts differences between inference samples and the corresponding results of the GAN model as inputs. **Scenario 2:** The detection model accepts inference samples as inputs. We train lightweight one-class models based on the state-of-the-art HRN approach [50] only from clean samples for each scenario, respectively, since the adversary has no information of the verification samples. The models project the outputs to a non-linear space $(0, 1)$ through a function $\text{sigmoid}(x) = 1/(1 + \exp^{-x})$. The detection result of normal samples is expected to be close to 1, while that of verification samples is expected to be close to 0. The backbone model in our experiment is ResNet34 [36], which is a common lightweight and powerful deep learning model in computer vision. Table 6 shows the performance of our anomaly detector under two scenarios. We adopt the AUC (Area Under the ROC Curve) metric: a higher AUC score means higher detection accuracy, while a score of 50 indicates the detector has similar performance as random guess. We observe that it is challenging to perform detection just based on the inference samples (Scenario 2) for all the methods. However, if the adversary adopts the difference between the inference samples and their corresponding outputs (Scenario 2), the anomaly detector can identify the verification samples based on AE-D and AE-I with very high accuracy, while the detection accuracy of CFP-* is still low. This demonstrates that our method is a stealthy approach for IP protection of GAN models.

D. Summary

Table 7 summarizes the comparisons of those methods from the above evaluations. There are five levels to assess each property of each method. AE-I is effective for fingerprinting the GAN model, but not robust enough against model pruning, fine-tuning or image transformations. AE-D cannot guarantee the high quality of verification samples on other GAN models, leading to low MSV scores. In Appendix F, we show the outputs of verification samples for three GANs, which reveal that AE-D is not a stable and general fingerprinting method. Besides, AE-I and AE-D are not stealthy, which gives an adversary more chances to detect the verification samples and manipulate the results. For our proposed scheme, CFP-AE is not good at resisting image transformations. With the introduction of the invisible backdoor technique for fingerprint embedding, CFP-iBDv1 and CFP-iBDv2 can significantly improve the effectiveness and persistency. The two novel loss function terms in CFP-iBDv2 can further increase the distinguishability between target and non-target GAN models. The three methods also give much better stealthiness in both the sample space and feature space.

Table 7: Assessment summary of each method. (Excellent > Good > Fair > Poor > Bad)

Method	Distinctness	Persistency		Stealthiness		
		Model trans.	Image trans.	Sample space	Feature space	Detection
AE-I	Excellent	Bad	Bad	Fair	Bad	Bad
AE-D	Poor	Fair	Fair	Poor	Bad	Bad
CFP-AE	Poor	Excellent	Good	Excellent	Good	Good
CFP-iBDv1	Fair	Excellent	Excellent	Excellent	Good	Good
CFP-iBDv2	Good	Excellent	Excellent	Excellent	Good	Good

VII. DISCUSSIONS

A. Limitations and Future Work

Ownership piracy attacks. Consistent with almost all the existing works [13]–[20], we do not consider ownership piracy attacks, where the adversary tries to embed his fingerprints into a model that has been previously fingerprinted by others. It is quite complicated to design a fingerprinting mechanism that can defeat such attacks. One potential approach is to introduce a third trusted party for fingerprint registration, which can increase the cost of the verification process. We leave this as future work.

Fingerprinting other types of GANs. This paper mainly focuses on the protection of image-to-image translation GANs. There are also other types of GANs, e.g., noise-to-image translation, models for synthesizing audios, texts, etc. We expect our scheme is general and extensible for those models as well. We will consider this as future work.

Protection against model extraction attacks. Although a few works about IP protection of classification models [18], [21], [51] evaluate model extraction attacks, they are not included in our threat model. The main reason is that extracting a GAN model requires the adversary to have much more significant amounts of computing resources than stealing a classification model, and is much easier to defeat by simply adding small scales of Gaussian noise to the output [52]. Besides, [52] only presents the attacks against noise-to-image GAN models, while the feasibility of extracting image-to-image models is unknown. How to design more resource-efficient model extraction attacks and evaluate the effectiveness of our scheme against them are interesting future directions.

Alternative schemes. We evaluate existing adversarial attacks for GAN models [37]–[41] as the fingerprint baselines, and show their limitations in stealthiness and persistency. An alternative direction is to seek for more robust and stealthy attacks for fingerprinting GANs. Adversarial attacks against GANs are much less studied, and we could not find a satisfactory solution. We urge researchers to explore this direction for both effective attacks and fingerprinting solutions. Nevertheless, our novel scheme provides a different perspective with off-the-shelf methodologies.

B. Related Works

We discuss some relevant works and highlight their differences from our solution.

Watermarking GANs. Compared to classification models, IP protection of GAN models is much less explored. To our best knowledge, the only work is [6], which designed a watermarking solution for GAN models. To embed a watermark into a protected GAN, the model owner needs to train the model from

scratch, which is less practical for an already trained GAN. As discussed in Section I, watermarking has the limitations of usability and applicability [17], [21], which can be solved by fingerprinting.

Using GANs for IP protection. Some works utilized GANs to enhance or defeat IP protection methods. For instance, [53] adopted GANs to generate watermarks for BERT language models. [54] applied GANs to identify and remove watermarks from classification models. Different from those works, our solutions focus on protecting GANs.

Meta learning for fingerprinting. Pan et al. [55] propose a meta-learning-based fingerprinting scheme, which is a task-agnostic framework independent of the tasks. They adopt a number of positive and negative suspect models, where the positive suspect models are derived from the protected model based on pruning, fine-tuning, and distillation, and the negative models are models different from the target model for different training data or model structures. Although their framework shows robustness against various attacks, we argue that it is not practical to protect GANs for commercial use. In Appendix H, we show the time to train a high-quality GAN. The heavy time cost makes this framework unrealistic in protecting state-of-the-art GANs.

Detecting and attributing GAN-generated images. Some works [56]–[58] leveraged fingerprints to detect GAN-generated images and trace their sources. However, they are not quite applicable to fingerprint GAN models for IP protection. For instance, [57], [58] require the model owner to modify the GAN model training process (e.g., training loss and training data) to have the capability of embedding fingerprints in the output images, which violates the requirement of model fingerprinting. In [56], the fingerprint in the output image is very sensitive to model transformations: “Even GAN training sets that differ in just one image can lead to distinct GAN instances [56].” As a result, an adversary can just use a different training set to fine-tune the target GAN model to invalidate the fingerprint. In contrast, our methods do not need to modify the model, and exhibit higher unremovability.

VIII. CONCLUSION

We propose a novel scheme to fingerprint GAN models to protect the IP. We introduce a classifier to construct a composite model with the protected GAN. From this composite model, we craft verification samples as the fingerprint, and embed it in the classifier. The classifier is able to distinguish the target and non-target models in a stealthy and robust manner. We design three fingerprinting methodologies based on generative adversarial examples and invisible backdoor attacks. Extensive evaluations validate the effectiveness of our designs.

REFERENCES

- [1] I. J. Goodfellow, J. Pouget-Abadie, M. Mirza, B. Xu, D. Warde-Farley, S. Ozair, A. C. Courville, and Y. Bengio, “Generative Adversarial Nets,” in *Proc. of the NeurIPS*, 2014, pp. 2672–2680.
- [2] C. Donahue, J. McAuley, and M. Puckette, “Adversarial audio synthesis,” *CoRR*, vol. abs/1802.04208, 2018.
- [3] T.-C. Wang, M.-Y. Liu, J.-Y. Zhu, A. Tao, J. Kautz, and B. Catanzaro, “High-resolution image synthesis and semantic manipulation with conditional gans,” in *Proc. of the CVPR*, 2018, pp. 8798–8807.
- [4] Z. He, W. Zuo, M. Kan, S. Shan, and X. Chen, “AttGAN: Facial attribute editing by only changing what you want,” *IEEE Transactions on Image Processing*, vol. 28, no. 11, pp. 5464–5478, 2019.
- [5] S. Reed, Z. Akata, X. Yan, L. Logeswaran, B. Schiele, and H. Lee, “Generative adversarial text to image synthesis,” in *Proc. of the ICML*, 2016, pp. 1060–1069.
- [6] D. S. Ong, C. S. Chan, K. W. Ng, L. Fan, and Q. Yang, “Protecting intellectual property of generative adversarial networks from ambiguity attacks,” in *Proceedings of the IEEE/CVF Conference on Computer Vision and Pattern Recognition*, 2021, pp. 3630–3639.
- [7] A. Brock, J. Donahue, and K. Simonyan, “Large scale GAN training for high fidelity natural image synthesis,” in *Proc. of the ICLR*, 2019.
- [8] G. Sun, S. Ding, T. Sun, and C. Zhang, “Sa-capsan: Using capsule networks with embedded self-attention for generative adversarial network,” *Neurocomputing*, vol. 423, pp. 399–406, 2021.
- [9] “Tiktok online image editor,” <https://www.tiktok.com/discover/online-image-editor>.
- [10] “Makegirlsmoe - create anime characters with ai,” <https://make.girls.moe>.
- [11] “Lunapic free online editor,” <https://www9.lunapic.com/editor/?action=beauty>.
- [12] Y. Uchida, Y. Nagai, S. Sakazawa, and S. Satoh, “Embedding watermarks into deep neural networks,” in *Proc. of the ICMR*, 2017, pp. 269–277.
- [13] Y. Adi, C. Baum, M. Cisse, B. Pinkas, and J. Keshet, “Turning your weakness into a strength: Watermarking deep neural networks by backdooring,” in *Proc. of the USENIX Security*, 2018, pp. 1615–1631.
- [14] E. Le Merer, P. Perez, and G. Trédan, “Adversarial frontier stitching for remote neural network watermarking,” *Neural Computing and Applications*, pp. 1–12, 2019.
- [15] Z. Li, C. Hu, Y. Zhang, and S. Guo, “How to prove your model belongs to you: A blind-watermark based framework to protect intellectual property of DNN,” in *Proc. of the ACSAC*, 2019, pp. 126–137.
- [16] J. Zhang, Z. Gu, J. Jang, H. Wu, M. P. Stoecklin, H. Huang, and I. Molloy, “Protecting intellectual property of deep neural networks with watermarking,” in *Proc. of the AsiaCCS*, 2018, pp. 159–172.
- [17] X. Cao, J. Jia, and N. Z. Gong, “IPGuard: Protecting the intellectual property of deep neural networks via fingerprinting the classification boundary,” *CoRR*, vol. abs/1910.12903, 2019.
- [18] N. Lukas, Y. Zhang, and F. Kerschbaum, “Deep neural network fingerprinting by conferrable adversarial examples,” *CoRR*, vol. abs/1912.00888, 2019.
- [19] S. Wang, X. Wang, P.-Y. Chen, P. Zhao, and X. Lin, “Characteristic examples: High-robustness, low-transferability fingerprinting of neural networks,” in *Proceedings of the Thirtieth International Joint Conference on Artificial Intelligence, IJCAI*, 2021, pp. 575–582.
- [20] S. Wang and C.-H. Chang, “Fingerprinting deep neural networks—a deepfool approach,” in *2021 IEEE International Symposium on Circuits and Systems (ISCAS)*. IEEE, 2021, pp. 1–5.
- [21] Z. Peng, S. Li, G. Chen, C. Zhang, H. Zhu, and M. Xue, “Fingerprinting deep neural networks globally via universal adversarial perturbations,” *arXiv preprint arXiv:2202.08602*, 2022.
- [22] S. Li, B. Z. H. Zhao, J. Yu, M. Xue, D. Kaafar, and H. Zhu, “Invisible backdoor attacks against deep neural networks,” *CoRR*, vol. abs/1909.02742, 2019.
- [23] F. Schroff, D. Kalenichenko, and J. Philbin, “FaceNet: A unified embedding for face recognition and clustering,” in *Proc. of the CVPR*, 2015, pp. 815–823.
- [24] J. Deng, J. Krause, and L. Fei-Fei, “Fine-grained crowdsourcing for fine-grained recognition,” in *Proc. of the CVPR*, 2013, pp. 580–587.
- [25] E. Gavves, B. Fernando, C. G. Snoek, A. W. Smeulders, and T. Tuytelaars, “Fine-grained categorization by alignments,” in *Proc. of the ICCV*, 2013, pp. 1713–1720.
- [26] Y. Choi, M. Choi, M. Kim, J.-W. Ha, S. Kim, and J. Choo, “StarGAN: Unified generative adversarial networks for multi-domain image-to-image translation,” in *Proc. of the CVPR*, 2018, pp. 8789–8797.
- [27] M. Liu, Y. Ding, M. Xia, X. Liu, E. Ding, W. Zuo, and S. Wen, “STGAN: A unified selective transfer network for arbitrary image attribute editing,” in *Proc. of the CVPR*, 2019, pp. 3673–3682.
- [28] A. Juels and M. Wattenberg, “A fuzzy commitment scheme,” in *Proc. of the CCS*, 1999, pp. 28–36.
- [29] C. Xiao, B. Li, J.-Y. Zhu, W. He, M. Liu, and D. Song, “Generating adversarial examples with adversarial networks,” in *Proc. of the IJCAI*, 2018, pp. 3905–3911.
- [30] W. Luo, X. Yang, X. Mo, Y. Lu, L. Davis, J. Li, J. Yang, and S.-N. Lim, “Cross-X Learning for Fine-Grained Visual Categorization,” in *Proc. of the ICCV*, 2019, pp. 8241–8250.

- [31] Z. Yang, T. Luo, D. Wang, Z. Hu, J. Gao, and L. Wang, "Learning to Navigate for Fine-Grained Classification," in *Proc. of the ECCV*, 2018, pp. 438–454.
- [32] F. Zhang, M. Li, G. Zhai, and Y. Liu, "Multi-branch and Multi-scale Attention Learning for Fine-Grained Visual Categorization," in *Proc. of the MMM*, 2021, pp. 136–147.
- [33] A. Dubey, O. Gupta, R. Raskar, and N. Naik, "Maximum-Entropy Fine Grained Classification," in *Proc. of the NeurIPS*, 2018, pp. 635–645.
- [34] A. Coladangelo, T. Vidick, and T. Zhang, "Non-interactive zero-knowledge arguments for qma, with preprocessing," in *Proc. of the Crypto*, 2020, pp. 799–828.
- [35] Z. Liu, P. Luo, X. Wang, and X. Tang, "Deep learning face attributes in the wild," in *Proc. of the ICCV*, 2015, pp. 3730–3738.
- [36] K. He, X. Zhang, S. Ren, and J. Sun, "Deep residual learning for image recognition," in *Proc. of the CVPR*, 2016, pp. 770–778.
- [37] Z. Fang, Y. Yang, J. Lin, and R. Zhan, "Adversarial attacks for multi target image translation networks," in *Proc. of the PIC*, 2020, pp. 179–184.
- [38] Q. Huang, J. Zhang, W. Zhou, W. Zhang, and N. Yu, "Initiative defense against facial manipulation," in *Proc. of the AAAI*, 2021, pp. 1619–1627.
- [39] N. Ruiz, S. A. Bargal, and S. Sclaroff, "Disrupting deepfakes: Adversarial attacks against conditional image translation networks and facial manipulation systems," in *Proc. of the ECCV Workshops*, 2020, pp. 236–251.
- [40] —, "Protecting against image translation deepfakes by leaking universal perturbations from black-box neural networks," *CoRR*, vol. abs/2006.06493, 2020.
- [41] C. Yeh, H. Chen, S. Tsai, and S. Wang, "Disrupting image-translation-based deepfake algorithms with adversarial attacks," in *Proc. of the WACV Workshops*, 2020, pp. 53–62.
- [42] A. Horé and D. Ziou, "Image quality metrics: Psnr vs. ssim," in *Proc. of the ICPR*, 2010, pp. 2366–2369.
- [43] N. Carlini and D. Wagner, "Towards evaluating the robustness of neural networks," in *Proc. of the S&P*, 2017, pp. 39–57.
- [44] P. Wang, D. Wang, Y. Ji, X. Xie, H. Song, X. Liu, Y. Lyu, and Y. Xie, "QGAN: quantized generative adversarial networks," *CoRR*, vol. abs/1901.08263, 2019.
- [45] T. D. Linh, S. M. Nguyen, and M. Arai, "Gan-based noise model for denoising real images," in *Proc. of the ACCV*, 2020, pp. 560–572.
- [46] Z. Hong, X. Fan, T. Jiang, and J. Feng, "End-to-end unpaired image denoising with conditional adversarial networks," in *Proc. of the AAAI*, 2020, pp. 4140–4149.
- [47] Z. Katzir and Y. Elovici, "Detecting adversarial perturbations through spatial behavior in activation spaces," in *Proc. of the IJCNN*, 2019, pp. 1–9.
- [48] K. Lee, K. Lee, H. Lee, and J. Shin, "A Simple Unified Framework for Detecting Out-of-Distribution Samples and Adversarial Attacks," in *Proc. of the NeurIPS*, 2018, pp. 7167–7177.
- [49] J. Wang, G. Dong, J. Sun, X. Wang, and P. Zhang, "Adversarial sample detection for deep neural network through model mutation testing," in *Proc. of the ICSE*, 2019, pp. 1245–1256.
- [50] W. Hu, M. Wang, Q. Qin, J. Ma, and B. Liu, "HRN: A holistic approach to one class learning," in *Proc. of the NeurIPS*, 2020.
- [51] H. Jia, C. A. Choquette-Choo, V. Chandrasekaran, and N. Papernot, "Entangled watermarks as a defense against model extraction," in *30th USENIX Security Symposium (USENIX Security 21)*, 2021, pp. 1937–1954.
- [52] H. Hu and J. Pang, "Stealing machine learning models: Attacks and countermeasures for generative adversarial networks," in *Annual Computer Security Applications Conference*, 2021, pp. 1–16.
- [53] S. Abdelnabi and M. Fritz, "Adversarial watermarking transformer: Towards tracing text provenance with data hiding," in *Proc. of the SP*, 2021, pp. 121–140.
- [54] H. Wang, M. Xue, S. Sun, Y. Zhang, J. Wang, and W. Liu, "Detect and remove watermark in deep neural networks via generative adversarial networks," *arXiv preprint arXiv:2106.08104*, 2021.
- [55] X. Pan, Y. Yan, M. Zhang, and M. Yang, "Metav: A meta-verifier approach to task-agnostic model fingerprinting," in *Proc. of the KDD*, 2022, pp. 1327–1336.
- [56] N. Yu, L. S. Davis, and M. Fritz, "Attributing fake images to gans: Learning and analyzing gan fingerprints," in *Proc. of the ICCV*, 2019, pp. 7556–7566.
- [57] N. Yu, V. Skripniuk, S. Abdelnabi, and M. Fritz, "Artificial fingerprinting for generative models: Rooting deepfake attribution in training data," *CoRR*, vol. abs/2007.08457, 2020.
- [58] N. Yu, V. Skripniuk, D. Chen, L. Davis, and M. Fritz, "Responsible disclosure of generative models using scalable fingerprinting," *CoRR*, vol. abs/2012.08726, 2020.
- [59] M. Abdalla, J. H. An, M. Bellare, and C. Namprempe, "From identification to signatures via the fiat-shamir transform: Minimizing assumptions for security and forward-security," in *Proc. of the Eurocrypt*, 2002, pp. 418–433.

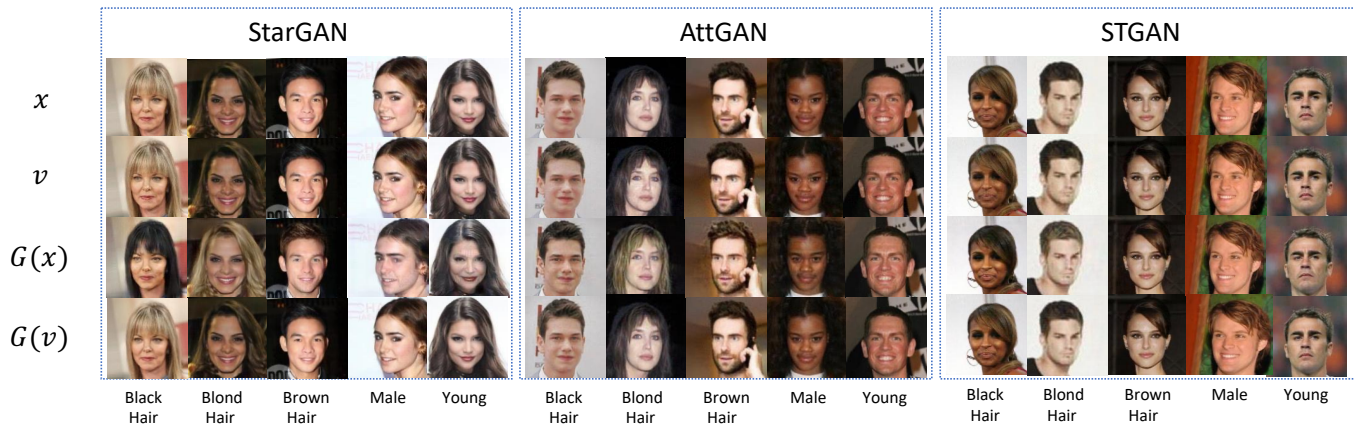


Fig. 1: Fingerprint visualization generated from AE-I for three GAN models with five edited attributes. (a) Clean sample x ; (b) Verification sample v ; (c) GAN output of clean sample $G(x)$; (d) GAN output of verification sample $G(v)$.

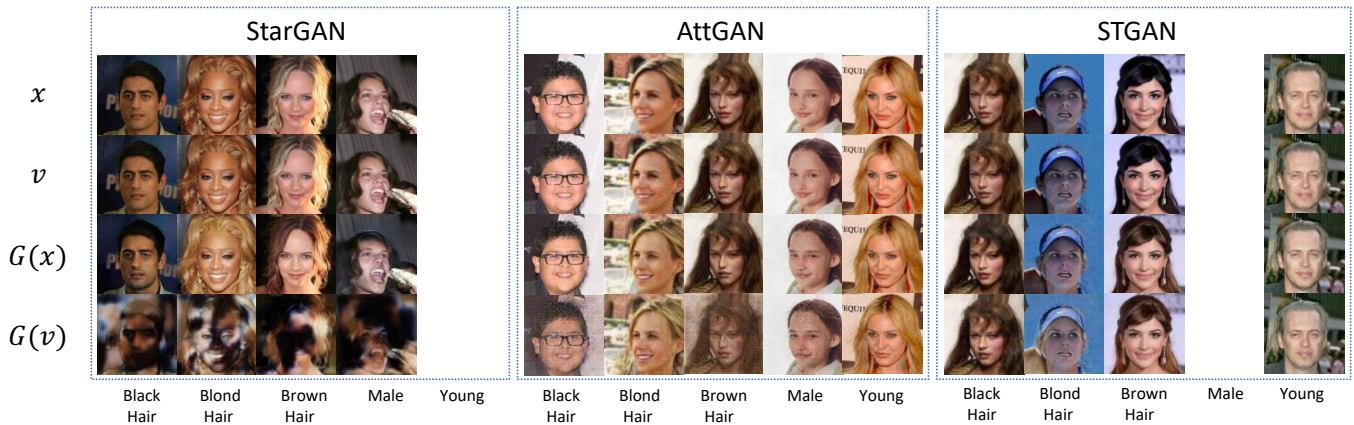


Fig. 2: Fingerprint visualization generated from AE-D for three GAN models with five edited attributes. (a) Clean sample x ; (b) Verification sample v ; (c) GAN output of clean sample $G(x)$; (d) GAN output of verification sample $G(v)$. Because there are no verification samples for some attributes, we leave these columns blank.

APPENDIX A SYMBOLS AND REMARKS

APPENDIX B ADVERSARY'S POWER

Let us introduce the adversary's capability in practice with more details. Firstly, when the model owner provides the service to others to use the model, the owner only needs the Generator of the GAN. The Discriminator of the GAN is deprecated, and any user cannot have the access to it, as the Discriminator may be deleted after the GAN is trained. It means that the adversary cannot steal both Generator and Discriminator, and the adversary can only steal the Generator at most. Secondly, the adversary does not have the ability to train a GAN to obtain the same performance as the stolen one, otherwise the adversary has no need to steal other's model. It means that the adversary does not have the ability to restore the Discriminator from the Generator. When fine-tuning the Generator, the adversary must have the Generator and the corresponding Discriminator at the same time. So the fine-tuning process is not possible in practice. However,

Table 1: Some important symbols and their remarks.

Symbol	Remarks
mk	a secret marking key
vk	a public verification key
$v^{(i)}$	a verification sample
$x^{(i)}$	a clean sample
D	a sample space
\bar{D}	a defined sample space
L	a label space
V, V'	verification sample sets
V_L, V'_L	verification label sets
F	a protected deep learning model
F^s	a suspicious model, whether it is stolen or not
G	the Generator of protected GAN
$G_{v^{(i)},j}, G_{x^{(i)},j}$	the j -th feature maps in G
$G(x)$	the accurate model outputs
$(G(x))^T$	the perturbed model outputs by the adversary
$\hat{G}(x)$	a set contains outputs of $G(x)$ and $(G(x))^T$
f^*	a ground-truth classifier projecting D to L
f	a normal classifier trained with \mathcal{O}^{f^*}
\hat{f}	f after fingerprinted
M	a composite deep learning model with f and G
\hat{M}	a fingerprinted composite deep learning model with \hat{f} and G
\mathcal{O}^{f^*}	an oracle truly answering each call to f^*
$\mathcal{A}, \mathcal{T}, \mathcal{S}$	PPT algorithms

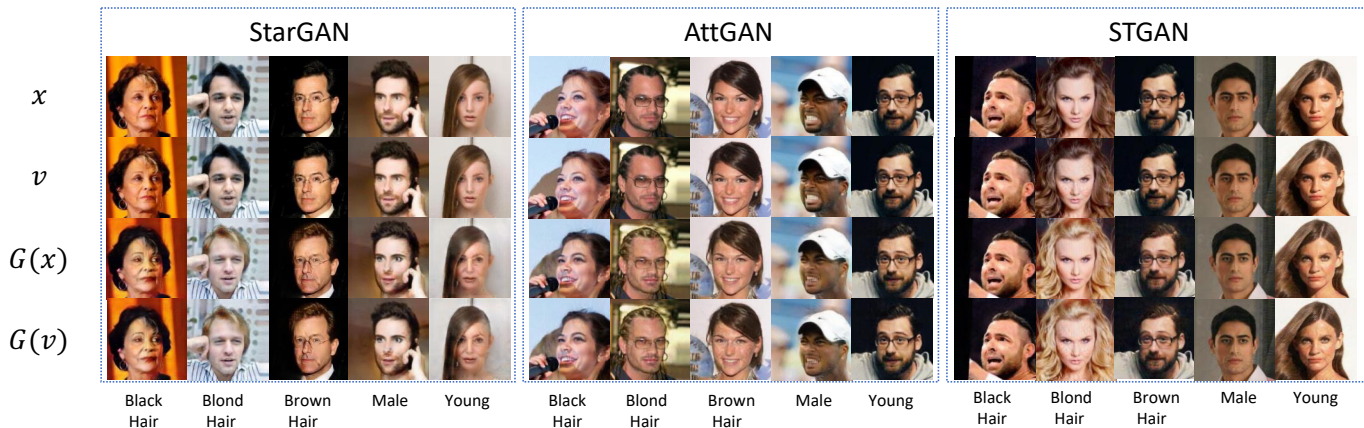


Fig. 3: Fingerprint visualization $CFP-\ast$ for three GAN models with five edited attributes. (a) Clean sample x ; (b) Verification sample v ; (c) GAN output of clean sample $G(x)$; (d) GAN output of verification sample $G(v)$.

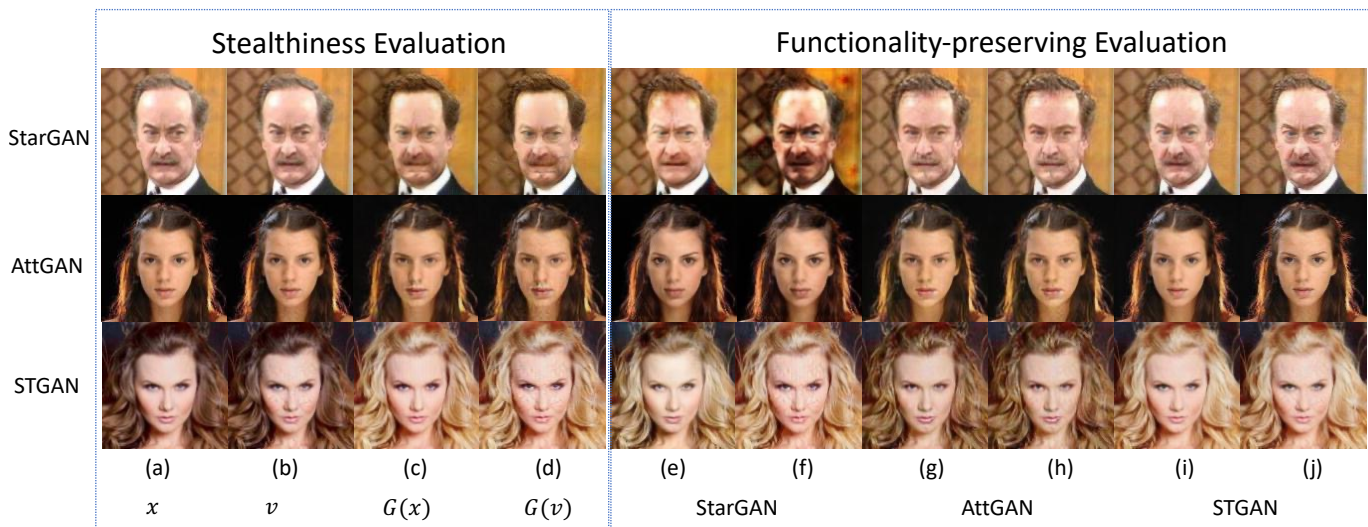


Fig. 4: Manipulated images from StarGAN, AttGAN, and STGAN. The column (e) edits attribute on x with StarGAN, the column (f) edits attribute on v with StarGAN, the column (g) edits attribute on x with AttGAN, the column (h) edits attribute on v with AttGAN, the column (i) edits attribute on x with STGAN, the column (j) edits attribute on v with STGAN.

the adversary may steal the Discriminator by some adaptive ways, such as stealing the hard disk storing the Discriminator. That is why fine-tuning the Generator is an adaptive attack in this paper. Further, let us consider a situation where the adversary prunes the Generator first and fine-tunes it later. For a PPT adversary, it is impossible to fine-tune a pruned Generator, as the Discriminator is no longer aligned with the pruned Generator. If using an unaligned Discriminator, it is easy to cause collapse in fine-tuning and make the Generator give worse results. A PPT adversary cannot find a set of parameters for the Discriminator to cooperate with the new Generator, otherwise the adversary can remove the fingerprint in the Generator directly by finding another set of parameters for it. As it is impossible, we do not consider this method in our experiments.

APPENDIX C PROOF OF THEOREM 1

(I) **Functionality-preserving.** By the definition of the algorithm F_{emb} , it outputs a model \hat{M} that satisfies

$$\Pr_{x \in D \setminus V} [f^*(\mathcal{G}(x)) \neq \text{Classify}(\hat{M}, x)] \leq \epsilon, \text{ and}$$

$$\Pr_{x \in V} [V_L(x) \neq \text{Classify}(\hat{M}, x)] \leq \epsilon.$$

As a result, given an error ϵ , \hat{M} classifies correctly for at least $(1 - \epsilon)|\mathcal{V}|$ elements in \mathcal{V} , which is consistent with the argument that Classify outputs 1 if \hat{M} disagrees with \mathcal{V} on at most $\epsilon|\mathcal{V}|$ elements.

(II) **Non-trivial ownership.** As defined in **Game 1**, if \mathcal{A} wants to win, he must guess the correct labels for a $(1 - \epsilon)$ fraction of V in advance, where we use (\tilde{V}, \tilde{V}_L) to represent the fingerprint set guessed by the adversary. Note that \mathcal{A} cannot change the selected \tilde{V} and \tilde{V}_L after seeing the model.

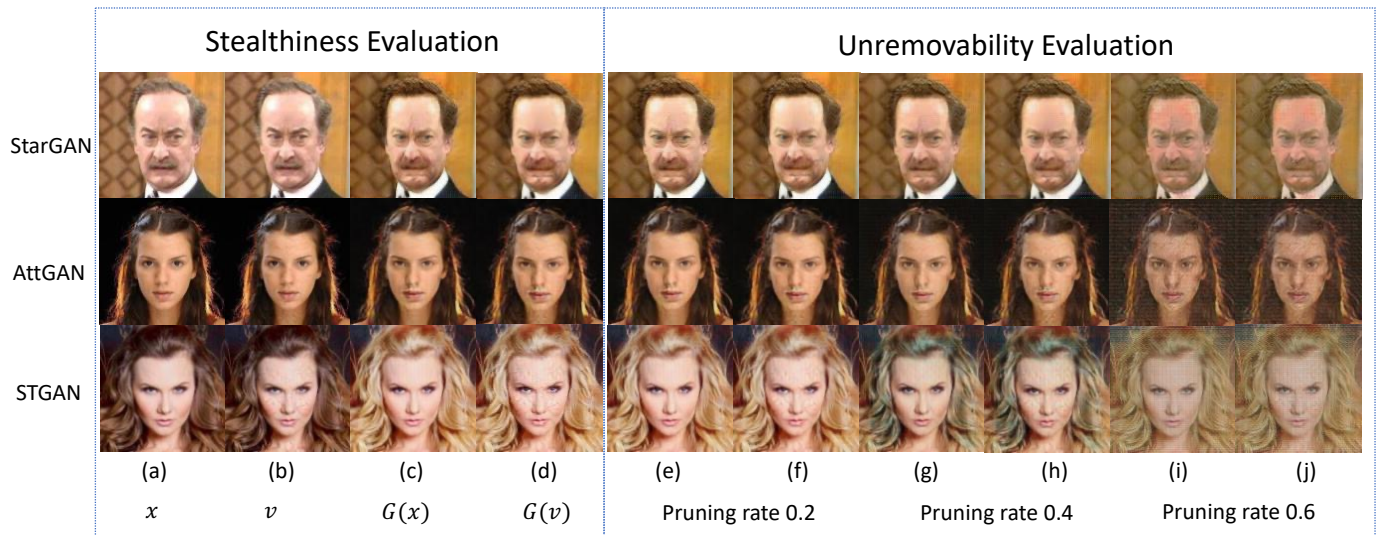


Fig. 5: Images manipulated by StarGAN, AttGAN and STGAN. The column (e) edits attributes on x with pruning rate 0.2, the column (f) edits attributes on v with pruning rate 0.2, the column (g) edits attributes on x with pruning rate 0.4, the column (h) edits attributes on v with pruning rate 0.4, the column (i) edits attributes on x with pruning rate 0.6, the column (j) edits attributes on v with pruning rate 0.6.

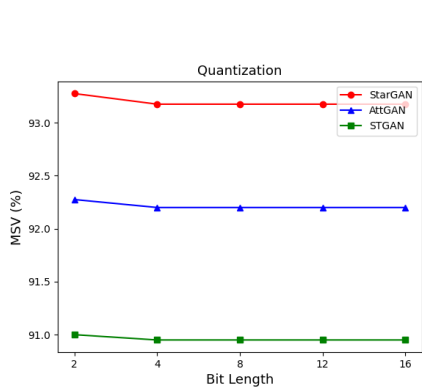


Fig. 6: MSV (%) of CFP-iBDv2 under different quantization scales. Bit Length stands for the truncation length for model parameters.

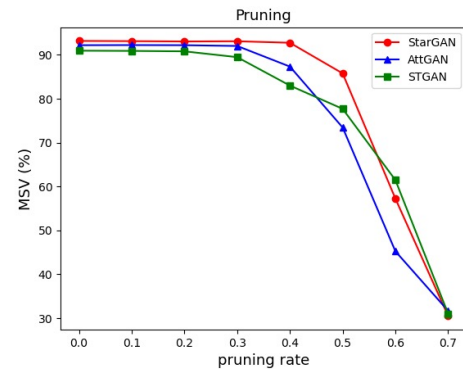


Fig. 8: MSV (%) of CFP-iBDv2 under different pruning rates.



Fig. 7: Outputs before and after model quantization. The first row is the outputs of the clean image and the verification image, respectively. The second row is the corresponding outputs after model quantization. Each column responds to the output of one Bit Length quantization model in Fig. 6.

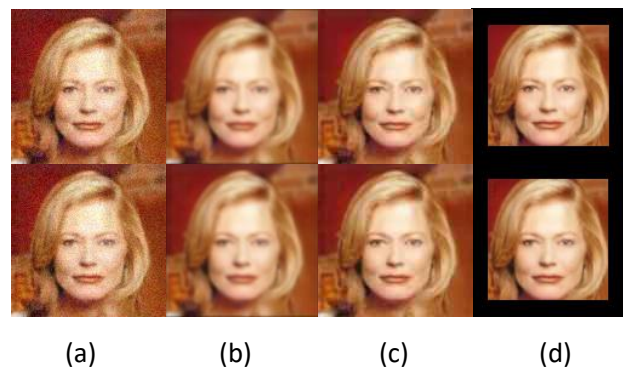


Fig. 9: Visualization of GAN output images corrupted by four types of image transformations. The first row is GAN outputs from clean images. The second row is GAN outputs from verification samples. (a) adding Gaussian Noise, (b) blurring, (c) JPEG compression, (d) centering cropping.

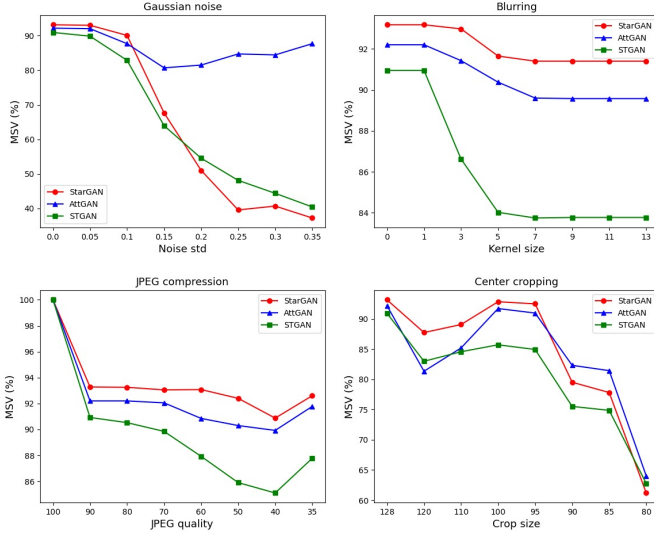


Fig. 10: MSV (%) of CFP-iBDv2 under different settings of transformations, which are applied on the outputs of the GAN.

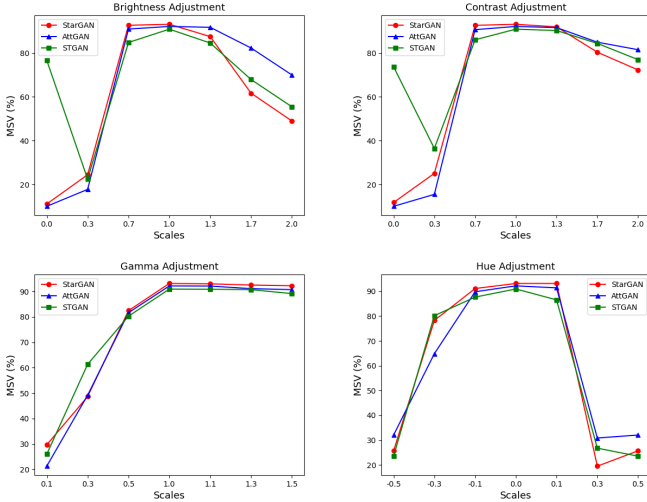


Fig. 11: MSV (%) of CFP-iBDv2 under different settings of transformations, which are applied on the outputs of the GAN.

This is determined by the binding property of the commitment scheme. On the other hand, since the algorithm **KeyGen** generates the set V in mk in a uniformly random space, $\tilde{m}k$ fixed by any algorithm \mathcal{A} has a negligible probability of intersection with V (due to the property of *multiple verification sample sets*). For simplicity, we assume that \tilde{V} and V will not intersect with each other. Now \mathcal{A} can generate \tilde{V} either from space in \bar{D} or outside D . Let $n_1 = |\bar{D} \cap \tilde{V}|$ and $n_2 = |\tilde{V}| - n_1$.

For the benefit of the adversary, we give a strong assumption that whenever M misclassifies the input $x \in \bar{D} \cap \tilde{V}$, the label of x is in \tilde{V}_L . However, since M is ϵ -accurate on \bar{D} , the ratio of incorrectly classified committed label is $(1 - \epsilon)$. We have $\epsilon n_1 < (1 - \epsilon)n_1$ for every choice $\epsilon < 0.5$. Because in our scheme, ϵ is usually much smaller than 0.5, the above inequality always holds. On the other hand, if all the values in \tilde{V} fall in $D \setminus \bar{D}$, according to the definition of the composite deep learning model, M will misclassify $\frac{|L|-1}{|L|}n_2$ elements in

expectation. We have $\epsilon n_2 < \frac{|L|-1}{|L|}n_2$ as $\epsilon < 0.5$ and $L \geq 2$. Since $\epsilon n = \epsilon n_1 + \epsilon n_2$, the error of \tilde{V} must be larger than ϵn .

(III) **Unremovability.** As defined in Section IV.A, we assume that no algorithms can generate an ϵ -accurate model N in the time t of f , where t is much smaller than the time required to train a model with the same accuracy as N using the algorithm **Train**. In addition, we assume that the time taken by the adversary \mathcal{A} to break the requirement of unremovability is approximately t . According to **Game 2**, \mathcal{A} will output an ϵ -accurate model when it is given the knowledge of \tilde{M} and vk , where at least a $(1 - \epsilon)$ fraction of the elements in V are classified correctly by \tilde{M} . We first prove that the adversary's realization of this is independent of the key vk . To achieve this, we construct a series of algorithms to gradually replace the verification samples in vk with other random values. Specifically, consider the following algorithm \mathcal{S} :

1. Generate $M \leftarrow \mathbf{Train}(\mathcal{O}^{f^*}, \mathcal{G})$ and $(mk, vk) \leftarrow \mathbf{KeyGen}()$.
2. Compute $\hat{M} \leftarrow \mathbf{FP}(M, mk)$ and run $(\tilde{V}, \tilde{V}_L) = \tilde{\mathcal{V}} \leftarrow \mathbf{F}_{\text{gen}}(\mathcal{O}^{f^*}, \mathcal{G})$, where $\tilde{V} = \{\tilde{v}^{(i)} | i \in [n]\}$, $\tilde{V}_L = \{\tilde{v}_L^{(i)} | i \in [n]\}$.
3. Set $c_v^{(1)} \leftarrow \mathbf{Com}(\tilde{v}^{(1)}, h_v^{(1)})$, $c_L^{(1)} \leftarrow \mathbf{Com}(\tilde{v}_L^{(1)}, h_L^{(1)})$, and $\tilde{vk} \leftarrow \{c_v^{(i)}, c_L^{(i)}\}_{i \in [n]}$. Then, compute $\tilde{M} \leftarrow \mathcal{A}(\mathcal{O}^f, \tilde{vk}, \hat{M})$.

This algorithm replaces the first element in vk with an independently generated random element, and then runs \mathcal{A} on it. Due to the statistical hiding property of **Com**, the output of \mathcal{S} is statistically close to the output of \mathcal{A} in the unremovability experiment. Therefore, we can further generate a series of hybrids $\mathcal{S}^{(2)}, \mathcal{S}^{(3)} \dots, \mathcal{S}^{(n)}$ to change the 2nd to n -th elements in vk in the same way. This means that the model \tilde{M} generated by the adversary \mathcal{A} must be independent of vk . Based on this, we consider the following algorithm \mathcal{T} :

1. Compute $(mk, vk) \leftarrow \mathbf{KeyGen}()$.
2. Run the adversary and compute $\tilde{N} \leftarrow \mathcal{A}(\mathcal{O}^f, M, vk)$.

According to the above hybrid argument, the running time of the algorithm \mathcal{T} is similar to that of \mathcal{A} , i.e., time t . Then it generates a model \tilde{N} which does not contain the fingerprint. However, this is contrary to the previous assumption about the persistence of strong fingerprints, i.e., \mathcal{T} must also generate an ϵ -accurate model given any model in the same time t .

(IV) **Unforgeability.** Suppose there is a polynomial time algorithm \mathcal{A} which can break the unforgeability requirement. We use such an algorithm to open the statistically hidden commitment. Specifically, we design an algorithm \mathcal{S} which uses \mathcal{A} as a subroutine. This algorithm trains a regular network (which can be fingerprinted through our scheme) and adds commitments into vk . Then, it will use \mathcal{A} to find openings for these commitments. \mathcal{S} works as follows:

1. Receive the commitments c from the challenger.
2. Generate $M \leftarrow \mathbf{Train}(\mathcal{O}^{f^*}, \mathcal{G})$ and $(mk, vk) \leftarrow \mathbf{KeyGen}()$.
3. Compute $\hat{M} \leftarrow \mathbf{FP}(M, mk)$.
4. Let $vk = \{c_v^{(i)}, c_L^{(i)}\}_{i \in [n]}$, set $\hat{c}_v^{(1)} = c$ and $\hat{c}_v^{(i)} = c_v^{(i)}$ for $i \in [n]$. Then, $\tilde{vk} \leftarrow \{\hat{c}_v^{(i)}, c_L^{(i)}\}$.
6. Compute $(\tilde{M}, \tilde{mk}) \leftarrow \mathcal{A}(\mathcal{O}^{f^*}, \tilde{vk}, \hat{M})$.
7. Let $\tilde{mk} = ((\{v^{(1)}, \dots, v^{(n)}\}, V_L), \{h_v^{(i)}, h_L^{(i)}\}_{i \in [n]})$. Then, if $\mathbf{Verify}(\tilde{mk}, \tilde{vk}, \tilde{M}) = 1$, output $v^{(1)}, h_v^{(1)}$. Otherwise, output \perp .

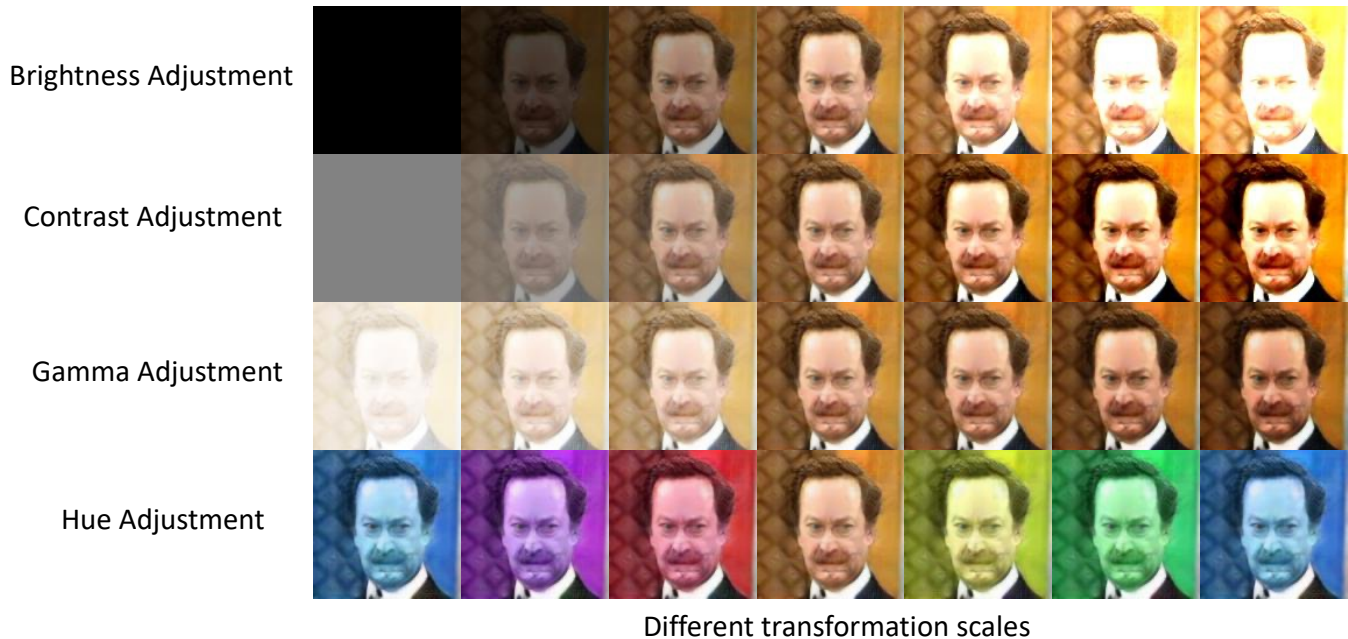


Fig. 12: Visualization results of outputs after applying image transformations on the outputs. The transformation scales are consistent with the values on the x-axis in Fig. 11.

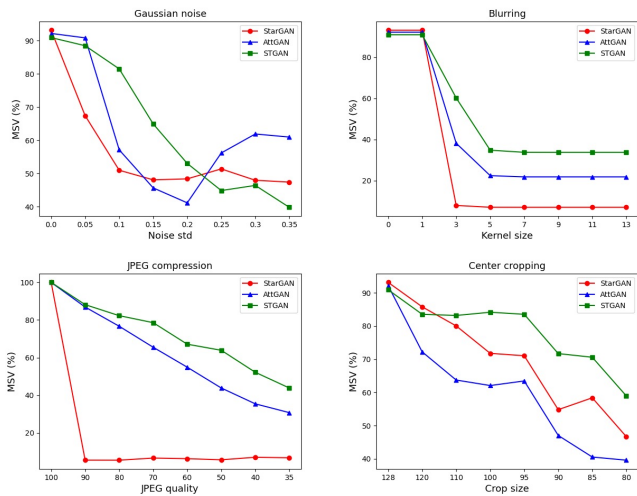


Fig. 13: MSV (%) of CFP-iBDv2 under different settings of transformations, which are applied on the inputs of the GAN.

We know that the commitment scheme is statistically hidden, so the input of \mathcal{A} is statistically indistinguishable from the input where \hat{M} is fingerprinted on all the committed values of vk . Therefore, this is statistically indistinguishable between the output of \mathcal{A} in \mathcal{S} and the output in the definition of unforgeability. If $\text{Verify}(\tilde{mk}, \hat{vk}, \tilde{M}) = 1$, it means that $\text{Open}(c, v^{(1)}, h_v^{(1)}) = 1$, so $v^{(1)}, h_v^{(1)}$ open the challenge commitment c . Since the commitment is statistically hidden (and the fingerprint we generate is independent of c), this will open c to another value with an overwhelming probability.

APPENDIX D

FROM PRIVATE TO PUBLIC VERIFIABILITY

As described previously, the algorithm **Verify** only allows verification by honest parties in a private way. This is evolved from the fact that the key mk will be known once **Verify** is run, which allows the adversary to retrain the model on the verification sample set. It is not a problem for the applications such as intellectual property protection, because there are trusted third parties in the form of judges. However, for practicality, we still hope to design a publicly verifiable method without limiting the number of repeated verifications. To achieve this, we first introduce some additional variables, and then use a powerful cryptographic primitive called the *zero-knowledge proof argument* [34], to convert our fingerprinting scheme from private verifiability to public verifiability. Specifically, we introduce a vector $\mathbf{e} \in \{0, 1\}^l$, where $\mathbf{e}|_0 = \{i \in [l] | \mathbf{e}[i] = 0\}$ and define $\mathbf{e}|_1$ accordingly. Given such a vector \mathbf{e} , a verification key $vk = \{c_v^{(i)}, c_L^{(i)}\}_{i \in [l]}$ can be split into

$$vk|_0^{\mathbf{e}} = \{c_v^{(i)}, c_L^{(i)}\}_{i \in \mathbf{e}|_0} \quad \text{and} \quad vk|_1^{\mathbf{e}} = \{c_v^{(i)}, c_L^{(i)}\}_{i \in \mathbf{e}|_1}$$

Similarly, given the marking key $mk = (\mathcal{V}, \{h_v^{(i)}, h_L^{(i)}\}_{i \in [l]})$ with $\mathcal{V} = (v^{(i)}, v_L^{(i)})$ we define

$$mk|_0^{\mathbf{e}} = (\mathcal{V}|_0^{\mathbf{e}}, \{h_v^{(i)}, h_L^{(i)}\}_{i \in \mathbf{e}|_0}) \quad \text{with} \quad \mathcal{V}|_0^{\mathbf{e}} = \{v^{(i)}, v_L^{(i)}\}_{i \in \mathbf{e}|_0}.$$

$mk|_1^{\mathbf{e}}$ is defined accordingly. Further, we assume that there is such a hash function $H : \{0, 1\}^{p(n)} \rightarrow \{0, 1\}^n$

A. Zero-Knowledge Arguments

The zero-knowledge argument is a technique that enables a prover \mathcal{PR} to convince the verifier \mathcal{VR} that a public statement

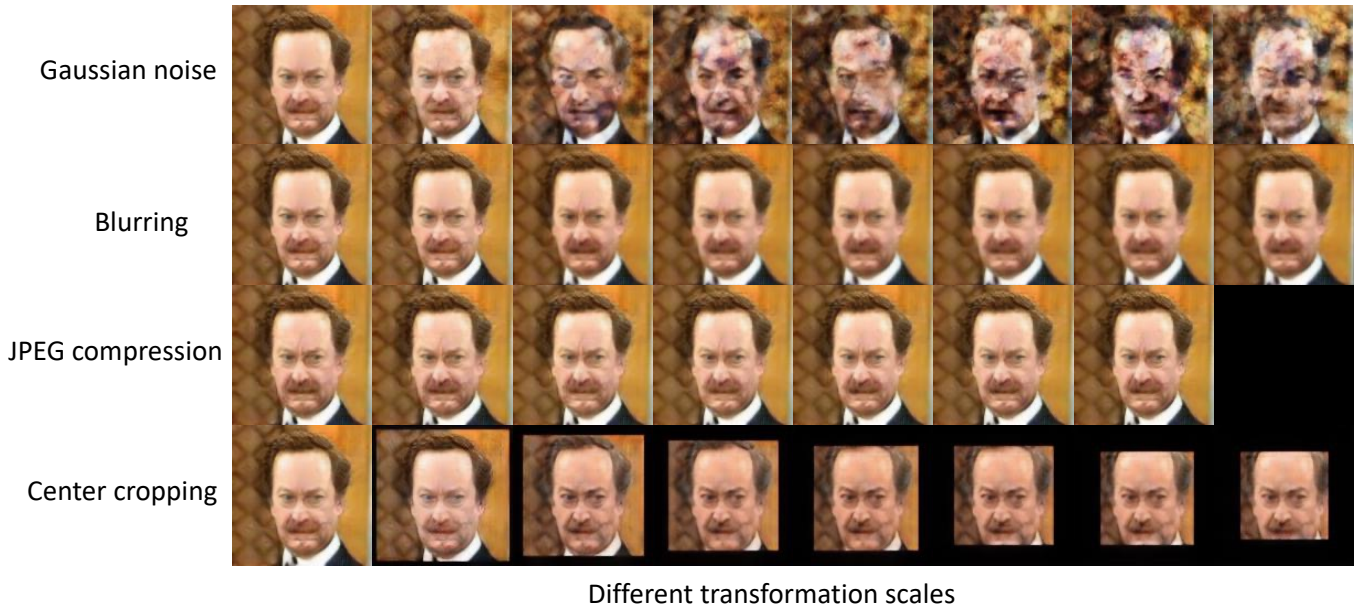


Fig. 14: Visualization results of outputs after applying image transformations on the inputs. The transformation scales are consistent with the values on the x-axis in Fig. 13.

is true without revealing more information. This core idea can be used to realize the public verifiability of fingerprints in this paper. Specifically, Let TM be the abbreviation of Turing machine, and iTM means an interactive TM, i.e., a Turing machine with a special communication tape. We define an NP language $L_R \subseteq \{0, 1\}^*$, where R is its related NP-relation, i.e., given a statement x and a witness w , if $x \in L_R$, then $(x, w) \in R$ and the TM exploited to define L_R outputs 1. We write $R_x = \{w | (x, w) \in R\}$ for the set of witness for a fixed x . Let \mathcal{PR} and \mathcal{VR} be a pair of PPT iTMs. For $(x, w) \in R$, \mathcal{PR} gets w as input while \mathcal{VR} gets an auxiliary random string $z \in \{0, 1\}^*$, where x is the input of both \mathcal{PR} and \mathcal{VR} . We use $\mathcal{VR}^{\mathcal{PR}(a)}(b)$ as the output of the iTM \mathcal{VR} given an input b when communicating with an instance of \mathcal{PR} with input a .

For language L , we say that $(\mathcal{PR}, \mathcal{VR})$ is an interactive zero-knowledge proof system if the following conditions hold: **Correctness.** For any $x \in L_R$, there exists a string w for every z , such that $\Pr[\mathcal{VR}^{\mathcal{PR}(x,w)}(x, z) = 1]$ is close to 1 with an overwhelming probability.

Soundness. For any $x \notin L_R$, $\Pr[\mathcal{VR}^{\mathcal{PR}(x,w)}(x, z) = 1]$ is negligible for every PPT iTM \mathcal{PR}^* and string w, z .

We say that an interactive system is computationally zero-knowledge for any $x \in L_R$, if there is a PPT simulator \mathcal{S} that satisfies the following condition for any PPT \mathcal{VR} .

$$\{\mathcal{VR}^{\mathcal{PR}(x,w)}(x, z)\}_{w \in R_x, z \in \{0, 1\}^*} \approx_c \{\mathcal{S}(x, z)\}_{z \in \{0, 1\}^*}$$

This means that we can obtain all the information by observing the protocol transcript from running a polynomial-time simulator \mathcal{S} , and the simulator does not know the witness w .

B. Technical Intuition

An intuitive way to build a publicly verifiable algorithm **PVerify** is to use a zero-knowledge argument system, where

the previously described algorithm **Verify**(mk, vk, M) is converted to a NP relation R . Unfortunately, such operations must fail due to Step 1 of **Verify**: testing whether the fingerprint \mathcal{V} is included in mk is actually the fingerprint defined above. Therefore, in the interactive demonstration system, we need to access the ground-truth function f . This requires human help first, but more importantly, it is only possible by exposing fingerprint elements.

In the following, we will give a different solution from the previous one, which requires an additional proof embedded in vk . This proof is used to show that it is an overwhelming probability that most elements in the verification key do indeed constitute a fingerprint. On this basis, we will design a different verification procedure based on the zero-knowledge system.

C. A Convincing Argument

If any random part of the elements released by the verification sample set is verified, it implies that most of the elements in the verification sample set are labeled wrongly, which constitute a fingerprint. To solve the problem of proof of misclassification, the cutting and selection technique is exploited. In this technique, the verifier \mathcal{VR} will ask the prover \mathcal{PR} to open a random subset of the committed inputs and labels in the verification key. Intuitively, if \mathcal{PR} makes a commitment for a large number of elements with correct labels (according to \mathcal{O}^f), then at least one of them intersects with the subset selected by \mathcal{VR} with an overwhelming probability, where this subset will be opened by \mathcal{PR} during the verification process. Hence, most of the remaining unopened commitments form a correct fingerprint.

To use the cutting and selection technique, the size of the fingerprint must contain $l > n$ elements. In this paper, we use

$l = 4n$. Then, we build a protocol between \mathcal{PR} and \mathcal{VR} as described below:

CnC(l):

1. \mathcal{PR} obtains a set of fingerprints with size l by running $(mk, vk) \leftarrow \mathbf{KeyGen}(l)$. Then, vk is sent to \mathcal{VR} . We define $mk = (\mathcal{V}, \{h_v^{(i)}, h_L^{(i)}\}_{i \in [l]}, vk = \{c_v^{(i)}, c_L^{(i)}\}_{i \in [l]}$.
2. \mathcal{VR} randomly selects a vector $\mathbf{e} \leftarrow \{0, 1\}^l$ and sends it to \mathcal{PR} .
3. \mathcal{PR} sends $mk|_{\mathbf{e}}$ to \mathcal{VR} .
4. \mathcal{VR} checks that for $i \in \mathbf{e}|_1$ that
 - a. $\mathbf{Open}(c_v^{(i)}, v^{(i)}, h_v^{(i)}) = 1$.
 - b. $\mathbf{Open}(c_L^{(i)}, v_L^{(i)}, h_L^{(i)}) = 1$, and
 - c. $v_l^{(i)} \neq f(G(v^{(i)}))$.

If \mathcal{PR} chooses exactly one element of the fingerprint in vk wrongly, this will be revealed to the honest \mathcal{VR} by the algorithm **CnC**(l) with a probability of $1/2$. In general, a cheating \mathcal{PR} can add up to n non-fingerprint elements to the vector $\mathbf{e}|_0$. Therefore, if the above verification is passed, there are at least n correct fingerprint elements in $vk|_0^{\mathbf{e}}$ with an overwhelming probability.

The above protocol can also be made non-interactive using the Fiat-Shamir transform [59]. Specifically, \mathcal{PR} can generate the vector \mathbf{e} by itself through the cryptographic hash function H to hash the verification key vk . This makes \mathbf{e} generated as if it were generated by the honest \mathcal{PR} , while it is sufficiently random by the guarantees of the hash function to allow the same analysis for cutting and selection. \mathcal{PR} can recalculate \mathbf{e} if it is obtained from the hash of vk , which also means that \mathbf{e} is generated after vk is constructed. Based on this, we can transform the above protocol from an interactive one to a non-interactive one with a new algorithm **PkeyGen**:

PkeyGen(l):

1. Run $(mk, vk) \leftarrow \mathbf{KeyGen}(l)$
2. Compute $\mathbf{e} \leftarrow H(vk)$.
3. Set $mk_p \leftarrow (mk, \mathbf{e})$, $vk_p \leftarrow (vk, mk|_{\mathbf{e}})$ and return (mk_p, vk_p) .

D. Concrete Public Verification Algorithm

Different from the previous private verification scheme, the algorithm **Mark** only uses the private subset $mk|_0^{\mathbf{e}}$ in mk_p during the publicly verifiable process, and the other parts remain unchanged. Therefore, a publicly verifiable solution follows the following structure: (i) \mathcal{VR} recalculates the challenger \mathbf{e} ; (ii) \mathcal{VR} verifies vk_p to ensure that all the elements in $vk|_1^{\mathbf{e}}$ form a valid fingerprint; (iii) \mathcal{PR} and \mathcal{VR} run the algorithm **Classify** on $mk|_0^{\mathbf{e}}$ using an interactive zero-knowledge argument system, and further test whether the conditions for fingerprints are held on M , $mk|_0^{\mathbf{e}}$ and $vk|_0^{\mathbf{e}}$.

For any model M , one can rewrite steps 1 and 3 of the algorithm **Verify** (utilizing M , **Open**, **Classify**) into a binary circuit \mathbf{C} . \mathbf{C} outputs 1 if the prover inputs $mk|_0^{\mathbf{e}}$ which can open $vk|_0^{\mathbf{e}}$ correctly and there are enough of these openings to satisfy the algorithm **Classify**. Both \mathcal{PR} and \mathcal{VR} can generate such a circuit \mathbf{C} and its construction does not involve private information. In the interactive zero-knowledge proof system, we define the relation R as a Boolean circuit

which outputs 1 where $x = \mathbf{C}$, $w = mk|_0^{\mathbf{e}}$ in the following protocol **PVerify**. **PVerify** will obtain M , $mk_p = (mk, \mathbf{e})$ and $vk_p = (vk, mk|_1^{\mathbf{e}})$, where $vk = \{c_v^{(i)}, c_L^{(i)}\}_{i \in [l]}$, $mk = (\mathcal{V}, \{h_v^{(i)}, h_L^{(i)}\}_{i \in [l]}$, and $\mathcal{V} = (v^{(i)}, v_L^{(i)})$ as inputs.

1. \mathcal{VR} computes $\mathbf{e}' \leftarrow H(vk)$. If \mathbf{e}' does not match $mk|_1^{\mathbf{e}}$ in vk_p , abort. Otherwise, continue assuming $\mathbf{e} = \mathbf{e}'$.
2. \mathcal{VR} checks that for $i \in \mathbf{e}|_1$ that
 - a. $\mathbf{Open}(c_v^{(i)}, v^{(i)}, h_v^{(i)}) = 1$.
 - b. $\mathbf{Open}(c_L^{(i)}, v_L^{(i)}, h_L^{(i)}) = 1$.
 - c. $v_l^{(i)} \neq f(G(v^{(i)}))$.
 If one of the checks fails, then \mathcal{VR} aborts.
3. \mathcal{PR} and \mathcal{VR} compute a circuit \mathbf{C} with input $mk|_0^{\mathbf{e}}$ that outputs 1 if for all $i \in \mathbf{e}|_0$:
 - a. $\mathbf{Open}(c_v^{(i)}, v^{(i)}, h_v^{(i)}) = 1$.
 - b. $\mathbf{Open}(c_L^{(i)}, v_L^{(i)}, h_L^{(i)}) = 1$. \mathcal{PR} and \mathcal{VR} also need to test that $\mathbf{Classify}(v^{(i)}, M) = v_L^{(i)}$ for all but $\epsilon|\mathbf{e}|_0$ elements.
4. Given the relationship R , \mathcal{PR} and \mathcal{VR} run a zero-knowledge argument using \mathbf{C} as a statement, where \mathcal{PR} 's secret input $mk|_0^{\mathbf{e}}$ is the witness, and \mathcal{VR} accepts if the argument is successful.

APPENDIX E

ATTRIBUTE SELECTION

When generating verification label set V_L for CFP-AE, we select the 5 attributes that are the easiest to be misclassified by the classifier for flipping. The selected attributes for each GAN model are listed in Table 2.

Table 2: Top-5 attributes for three GANs in verifying the model with CFP-AE.

GAN	Selected fingerprinting attributes
AttGAN	Smiling, BagsUnderEyes, Attractive, MouthSlightlyOpen, HighCheekbones
StarGAN	Smiling, Male, Young, WearingNecklace, Attractive
STGAN	BigNose, Young, Smiling, BagsUnderEyes, HighCheekbones

APPENDIX F

VERIFICATION SAMPLES OF DIFFERENT SCHEMES

In this section, we show the verification samples of AE-I, AE-D and CFP-* in Fig. 1, Fig. 2 and Fig. 3, respectively. For AE-I, it is clear that all GANs can generate high quality outputs from the verification samples, and they are similar visually. However, AE-D does not have the same performance on AttGAN and STGAN as on StarGAN. Because AttGAN and STGAN have more stable generation structures, which means generating disrupted images by them are more difficult. On the other hand, AE-D still achieve a very high SSIM on AttGAN and STGAN, which is shown in Section VII.C, indicating it is not a stable and general fingerprinting scheme.

APPENDIX G

HIGH-RESOLUTION FACIAL IMAGES OF CFP-*

In our experiments, we evaluate the performance of our proposed method by verifying whether the generated fingerprints satisfy the *functionality-preserving*, *unremovability*, and

stealthiness properties. Here, we present the high-resolution of GAN outputs of CFP-* in suffering various degradation, including model compression and corruptions with common image transformations.

A. Verification Samples after Different GANs

In Fig. 4, we show our CFP-iBDv2 verification samples’ outputs for different GANs. The columns from (e) to (j) indicate the output images from different models manipulated on both clean samples and verification samples. The verification samples do not decrease other GANs outputs’ quality in most cases. The outputs of verification samples look similar to outputs of clean samples. It means our CFP-iBDv2 has good functionality-preserving property.

B. Verification Samples suffer Degradation

In evaluating the unremovability of our proposed method, we mainly consider the two different degradation, model transformations and common image transformations. Here, we will give more results under different degrees of degradation. **Model Transformations.** In evaluating the unremovability against model compression (i.e., pruning), we explore the effectiveness of our method when the GAN model is compressed in various levels. In Fig. 5, the column (e) to (h) indicate the manipulated images with compressed models when the pruning rate is not larger than 0.4. We can find that the GAN’s outputs maintain a high-quality visualization, thus the pruning rate no more than 0.4 is an appropriate setting in our experiment. Furthermore, if the pruning rate is higher, when it is 0.6, the outputs is not satisfying for a user. We further compare more experimental results under various pruning rates showing in the Fig. 8. When the pruning rate is smaller than 0.5, the MSV (%) is high enough to pass the verification (the threshold is 0.8). With the pruning rate increasing, the MSV (%) will drop slowly at first and decrease significantly after the pruning rate is higher than 0.5. Because the outputs’ quality is not good enough for the backdoor classifier to recognize the triggers. We apply model quantization on GANs based on model parameter truncation, which means we keep model paramters with a specific length. After different scales’ quantization, our method can successfully verify the fingerprinted GAN, which can be found in Fig. 6. The visulization results in Fig. 7 indicates that under model quantization, GANs can generate high quality results.

Image Transformations. The GAN’s outputs will always be corrupted by various image transformations when spreading in the social models. Fig. 9 presents the visualization of GAN’s outputs by employing four different types of common image transformations, including adding *Gaussian noises*, *blurring*, *JPEG compression*, and *centering cropping*. Here, the parameters of these transformations are described in Section VII.B. In Fig. 10, we show the MSV (%) under different transformation magnitudes, which transformation applies on the outputs of the GAN. Clearly, our CFP-iBDv2 is robust under blurring and compression. These two transformations have trivial influence during the verification process. As for adding Gaussian noise, CFP-iBDv2 is robust on the AttGAN, and when the noise

std is higher than 0.1, the verification process will fail on the StarGAN and STGAN. Center cropping can significantly decline the completeness of backdoor triggers, resulting in the verification failure. Our CFP-iBDv2 can still work when the cropping size is bigger than 90, which is an excellent result.

Additionally, we explore unseen image transformations’ effects on our verification classifier. In Fig. 11, we compare four unseen image transformations, i.e., brightness adjustment, contrast adjustment, gamma adjustment and hue adjustment. For each adjustment, we consider different transformation intensities, and the outputs after each can be found in Fig. 12. The results confirm that our method can defend against these unseen transformations even we do not use them to train our verification classifier.

Furthermore, in Fig. 13, we show the MSV under different transformation magnitudes of CFP-iBDv2, in which transformation applies on the inputs of GANs. The MSV in these figures is significantly low, which is because when we add image transformations on the inputs, the outputs of the GAN lost most of details which contain the fingerprint information, which can be found in Fig. 14, especially under Gaussian noise and compression, which introduce non-trivial noise to replace our backdoor perturbation. We believe that this type of image transformations will not be used in practice as a defense.

After the comprehensive experiments on model pruning and image transformations, our CFP-iBDv2 shows impressive *functionality-preserving*, *unremovability*, and *stealthiness*. It can defend against gentle and medium image modification and model compression. More than that, its outputs are visually indistinguishable for humans.

APPENDIX H TIME COST COMPARISON

Training a high-quality GAN will cost a lot of time. For example, training a StarGAN, used in our paper, on one V100 will cost about one week to achieve good performance. Training a StyleGAN, which is a popular generative model, on 8 GPUs will cost one week to generate high resolution images⁸. Therefore, protecting the GAN is vital. Compared with the training cost, generating one image as fingerprint to verify the GAN only needs several minutes, depending on the GAN itself.

⁸<https://github.com/NVlabs/stylegan>